Electronic Supplementary Material (ESI) for CrystEngComm.

Supplementary Information

Evaluating the role of urea-like motif in enhancing the thermal and mechanical strength of supramolecular gels

Daníel Arnar Tómasson, Dipankar Ghosh, M.R. Prathapachandra Kurup, Matthew T. Mulvee and Krishna K. Damodaran*

Table of content

1. Gelation studies

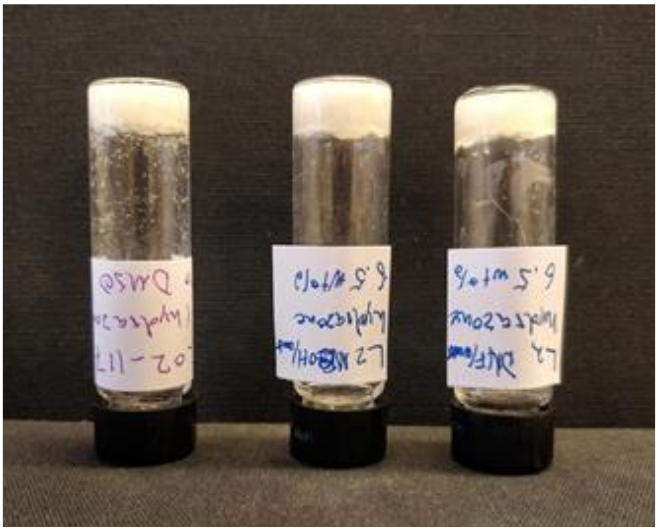

Fig. S1: Gels of **HL_1** at 5.0 wt% in 1:1 (v/v) mixture of DMSO/water (left), DMF/water (middle) and MeOH/water (right).

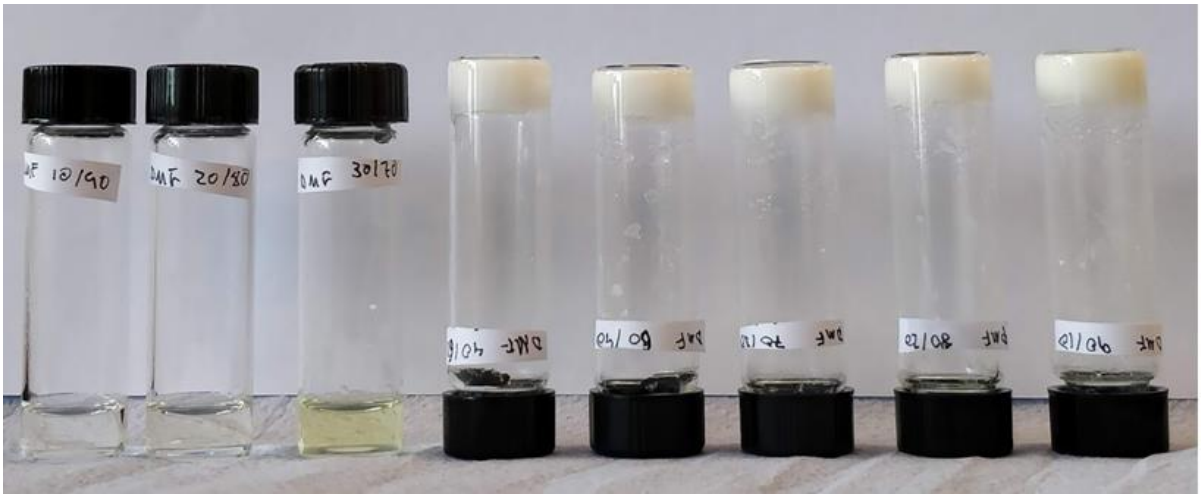

Fig. S2: Gels formed by varying ratios of HL_2 at 1.0 wt% in DMF/water (v/v): from 10% water/90% DMF (left) to 90% water/10% DMF (right).

Table S1: Gelation experiment of **HL_2** at 2.0 wt% in various solvents

Solvent (1.0 mL)	Initial Observation	Observation after 24 h
THF	Solution	Solution
EtOH	Solution	Solution
MeOH	Solution	Solution
Acetone	Solution	Solution
IPA	Solution	Gel*
Acetonitrile	Solution	Gel
Dioxane	Solution	Solution
DMF	Solution	Solution
DMA	Solution	Solution
DMSO	Solution	Solution

*Gel was obtained at 1.0 wt%.

Table S2: MGC of **HL_1**

Solvent	**HL_1**
MeOH/water	5.0
DMF/water	5.0
DMSO/water	3.99

2. Scanning electron microscopy

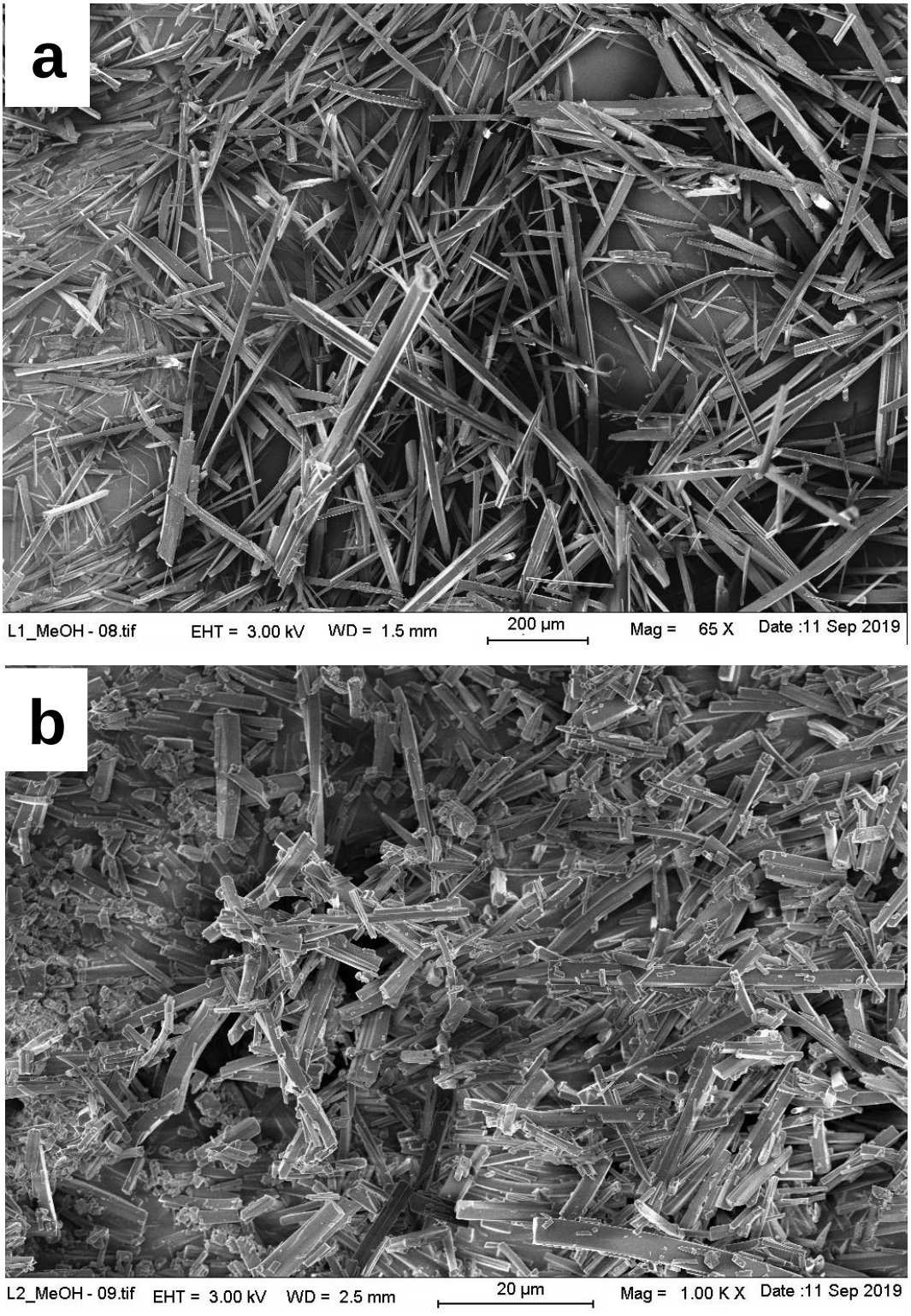

Fig. S3: SEM images of the xerogels of (a) **HL_1** (5.0 wt%) and (b) **HL_2** (2.0 wt%) from MeOH/water (1:1 v/v).

3. X-ray Crystallography

Table S3: Crystal data

Parameter	HL_2	1	2	4	5	7
Empirical formula	$C_{18}H_{15}N_5O$	$C_{36}H_{26}N_8O_2Zn$	$C_{40}H_{32}Cd_2N_8O_6,2(H_2O)$	$C_{36}H_{26}CdN_8O_2$	$C_{36}H_{30}N_{12}O_8Zn$	$C_{18}H_{15}CdCl_2N_5O$
Colour	Yellow	Yellow	Yellow	Yellow	Yellow	Yellow
Formula weight (g mol^{-1})	317.35	668.02	981.57	715.05	824.09	500.65
Crystal size (mm)	0.3 x 0.04 x 0.03	0.43 x 0.24 x 0.1	0.38 x 0.24 x 0.18	0.19 x 0.115 x 0.06	0.2 x 0.18 x 0.14	0.32 x 0.26 x 0.12
Crystal system	monoclinic	monoclinic	tetragonal	monoclinic	monoclinic	monoclinic
SPACE GROUP	*P2$_1$/n*	*C2/c*	*I4$_1$/a*	*P2$_1$/n*	*P2$_1$/c*	*P2$_1$/n*
a (Å)	3.84640(10)	18.2863(11)	29.630(2)	15.3928(10)	13.4129(8)	8.1129(5)
b (Å)	11.0679(3)	11.3902(6)	29.630(2)	10.6783(7)	18.8966(12)	14.5881(8)
c (Å)	35.2718(9)	30.447(2)	8.9973(7)	19.4846(12)	15.1602(9)	15.9877(9)
α (°)	90	90	90	90	90	90
β (°)	91.8120(10)	106.745(2)	90	96.349(2)	113.177(2)	93.220(2)
γ (°)	90	90	90	90	90	90
Volume (Å3)	1500.83(7)	6072.7(6)	7899.1(14)	3183.0(4)	3532.4(4)	1889.19(19)
Z	4	8	8	4	4	4
$d_{calc.}$(g cm^{-3})	1.404	1.461	1.651	1.492	1.550	1.760
F(000)	664	2752	3936	1448	1696	992
μ K_α (mm^{-1})	μ CuK_α 0.745	μ MoK_α 0.858	μ MoK_α 1.140	μ CuK_α 5.874	μ MoK_α 0.769	μ MoK_α 1.457
Temperature (K)	150(2)	150(2)	150(2)	295(2)	121(2)	150(2)
Reflections collected/unique/ observed [I > 2σ(I)]	30671/3206/2729	83125/8546/ 7283	118452/5572/4772	64208/6238/5831	105076 /9280/ 7355	56749/ 6321/5451
Data/restraints/parameters	3206/0/225	8546/0/424	5572/0/271	6238/0/424	9280/0/514	6321/0/244
Goodness of fit	1.062	1.018	1.095	1.054	1.018	1.025
Final R indices [I>2σ(I)]	R_1 = 0.0460, wR_2 =0.1096	R_1 = 0.0341 wR_2 =0.0842	R_1 = 0.0355 wR_2 = 0.0859	R_1 = 0.0279 wR_2 = 0.0693	R_1 = 0.0338 wR_2 = 0.0744	R_1 = 0.0189 wR_2 =0.0435
R indices (all data)	R_1 =0.0562, wR_2 = 0.1155	R_1 =0.0447 wR_2 = 0.0880	R_1 = 0.0449 wR_2 = 0.0888	R_1 = 0.0299 wR_2 = 0.0708	R_1 = 0.0533 wR_2 = 0.0794	R_1 = 0.0269 wR_2 = 0.0456

Table S4: Hydrogen bonding table

Donor—H···Acceptor	D—H/Å	H···A/Å	D···A/Å	∠D—H···A/°	Symmetry operation
Complex 1					
C(21)—H(21)···N(36)	0.95	2.59	3.360(2)	139	-1/2+x,-1/2+y,z
C(43)—H(43)···O(46)	0.95	2.41	3.249(2)	147	1/2-x,1/2+y,3/2-z
Complex 2					
O28 —H28A···O28	0.86(4)	2.00(4)	2.841(4)	167(4)	1/4+y,5/4-x,1/4+z
O28 —H28B···O27	0.83(5)	1.90(6)	2.729(4)	175(5)	x,y,z
C10 —H10 ···O24	0.95	2.33	3.069(4)	134	2-x,1-y,-z
Complex 4					
C(9)—H(9)···O(23)	0.93	2.56	3.461(3)	163	1-x,1-y,1-z
C(27)—H(27)···O(23)	0.93	2.33	3.203(3)	156	3/2-x,1/2+y,3/2-z
Complex 5					
N(15)—H(15)···O(55)	0.88	2.24	2.960(2)	139	x,y,z
N(17)—H(17)···O(55)	0.88	1.87	2.723(2)	164	x,y,z
N(39)—H(39)···O(49)	0.88	1.90	2.779(2)	172	x,y,z
N(41)—H(41)···O(52)	0.88	1.93	2.793(2)	167	x,y,z
C(2)—H(2)···O(49)	0.95	2.37	3.262(2)	157	-x,1-y,1-z
C(28)—H(28)···O(53)	0.95	2.43	3.220(3)	141	-1+x,y,z
C(28)—H(28)···O(56)	0.95	2.52	3.446(3)	166	-1+x,y,z
C(35)—H(35)···O(56)	0.95	2.38	3.319(2)	172	-1+x,1/2-y,-1/2+z
C(43)—H(43)···O(52)	0.95	2.55	3.273(2)	133	x,y,z
Complex 7					
N17 —H17···Cl2	0.88	2.33	3.1514(11)	156	1-x,1-y,1-z
C11 —H11···Cl1	0.95	2.75	3.6947(15)	171	1/2-x,-1/2+y,1/2-z
C21 —H21···Cl2	0.95	2.81	3.7132(15)	160	1/2-x,-1/2+y,3/2-z

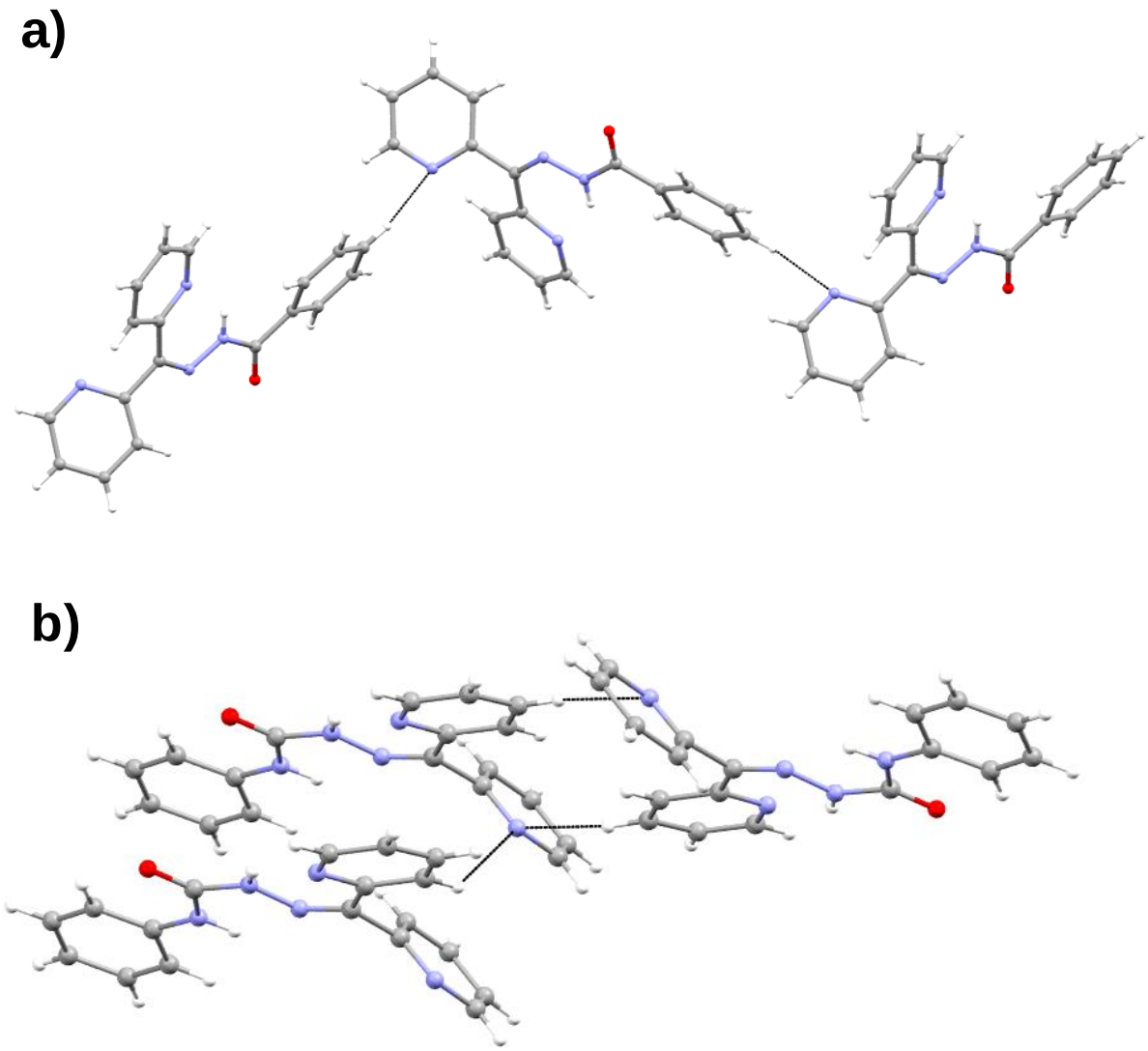

Fig. S4: Illustration of C-H⋯N interactions observed in the crystal structures of (a) **HL_1** and (b) **HL_2.**

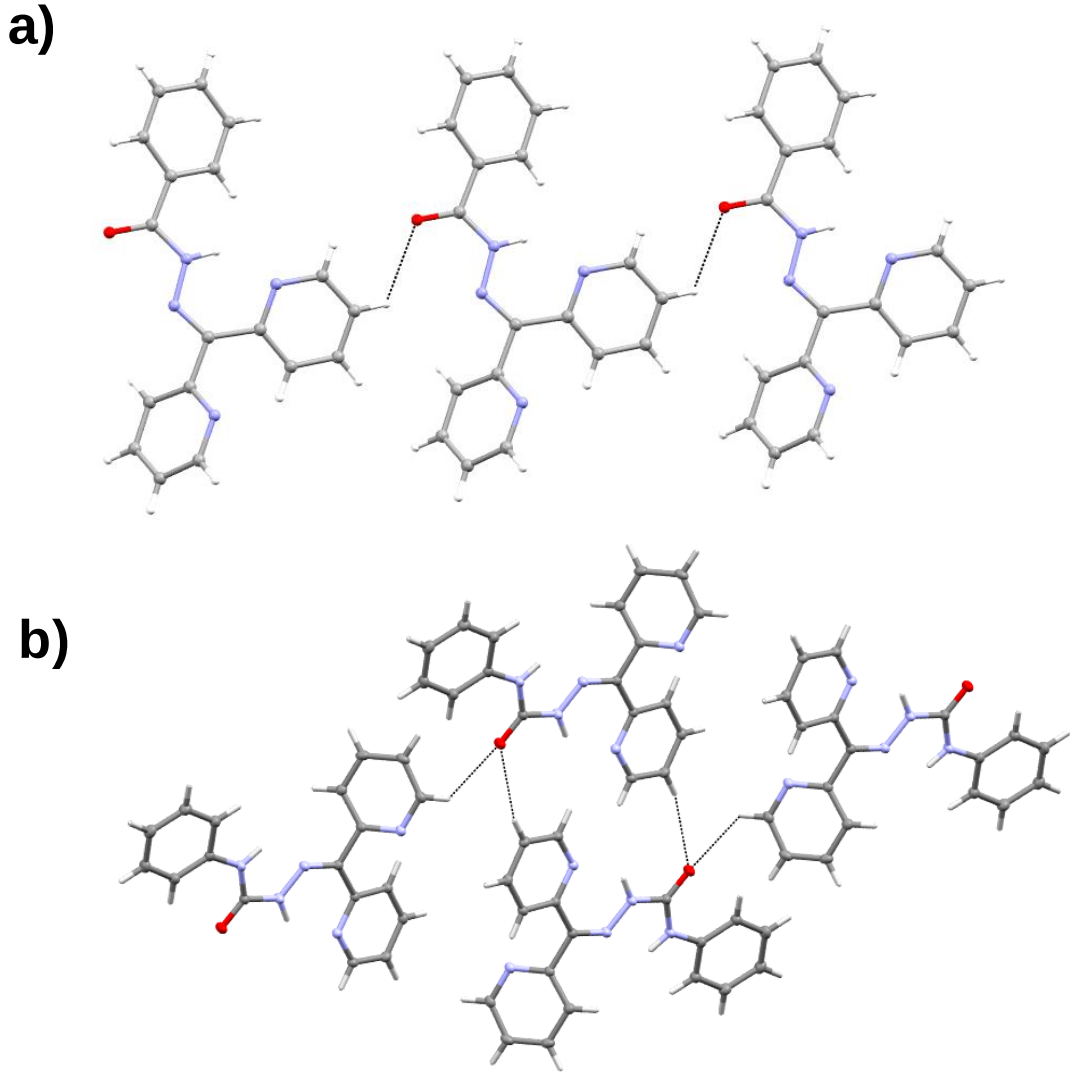

Fig. S5: Illustration of C-H···O interactions observed in the crystal structures of (a) **HL_1** and (b) **HL_2**.

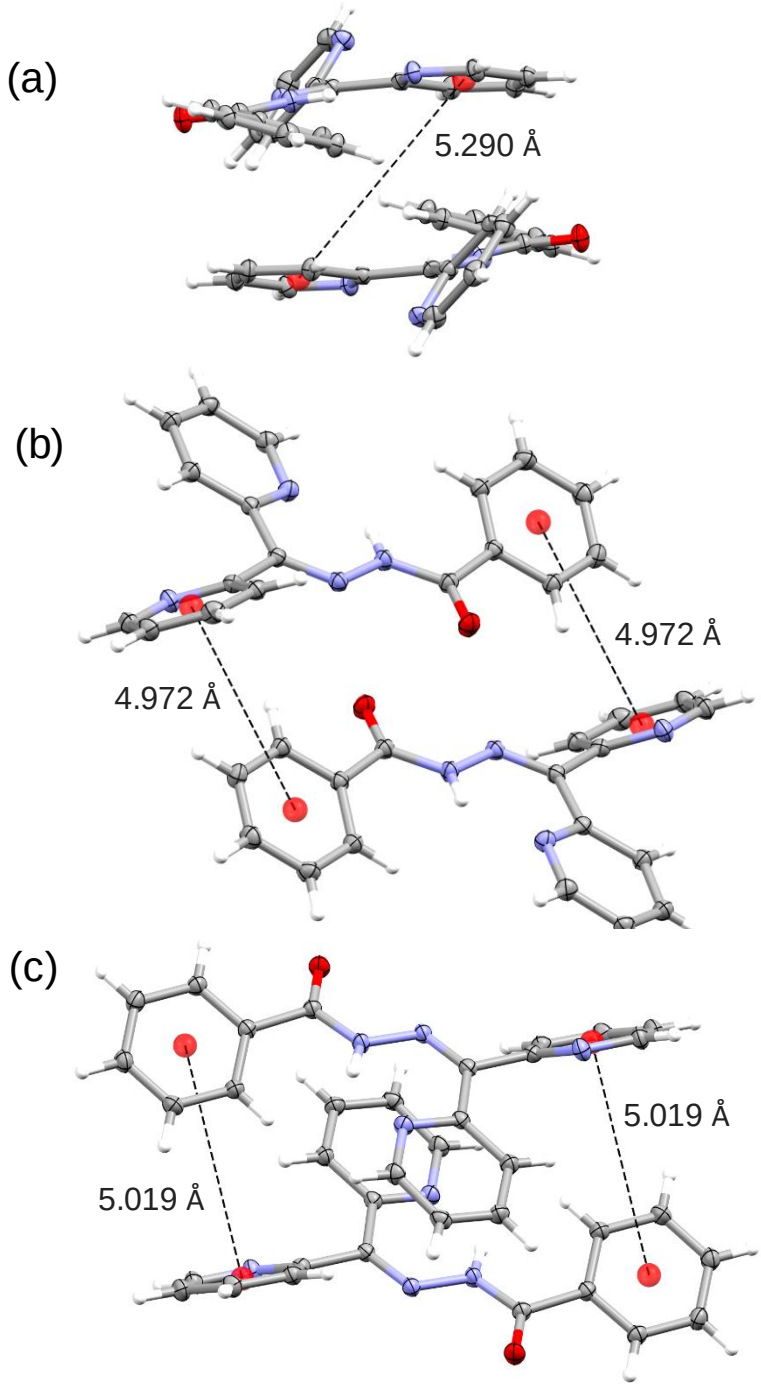

Fig. S6: Various π–π interactions observed in **HL_1** (a) offset and (b) & (c) edge to face (T-shaped) interactions.

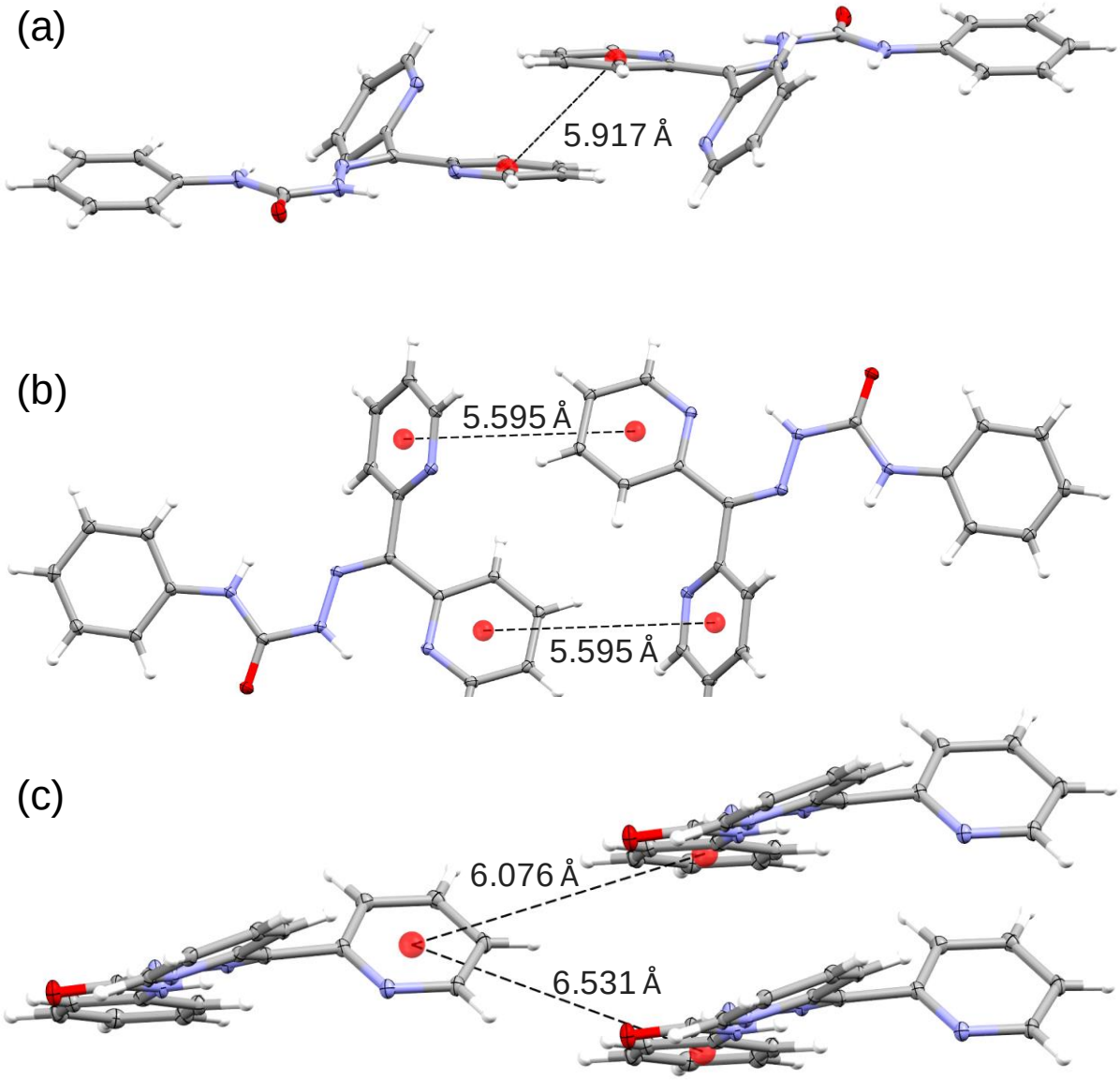

Fig. S7: Various non-bonding interactions observed in **HL**$_2$ (a) offset π–π interaction and (b) & (c) edge to face (T-shaped) π–π interactions.

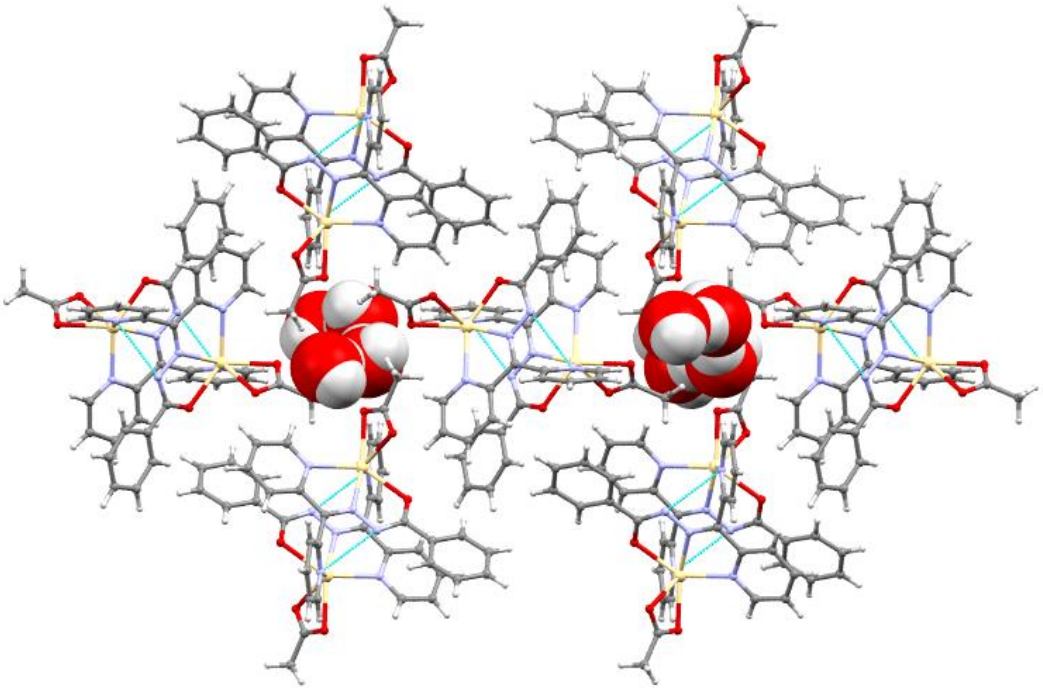

Fig. S8: Boxed dimers of complex **2**.

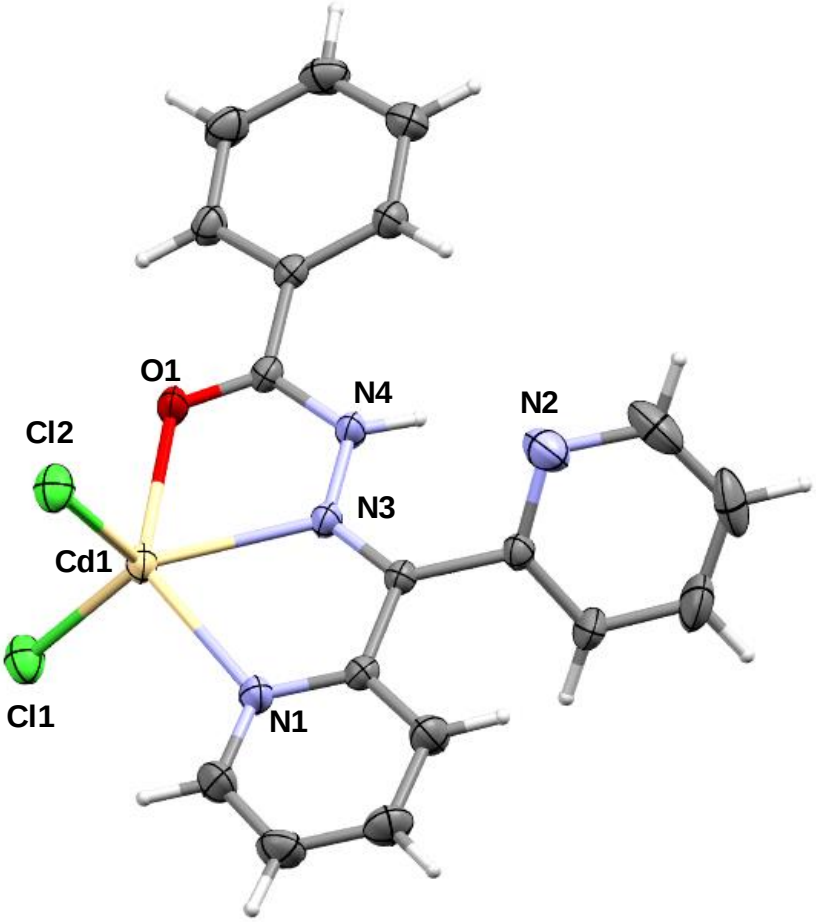

Fig. S9: Molecular structure of complex **3**.

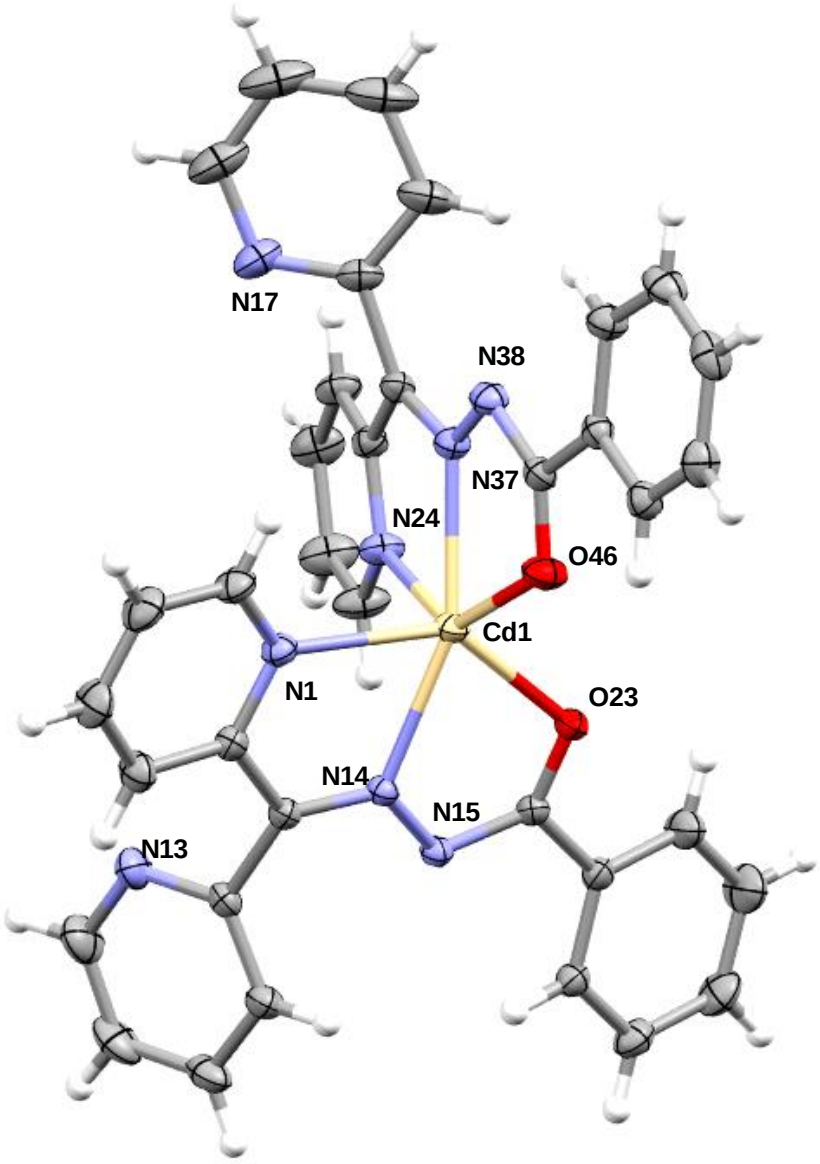

Fig. S10: Molecular structure of complex **4**.

4. NMR

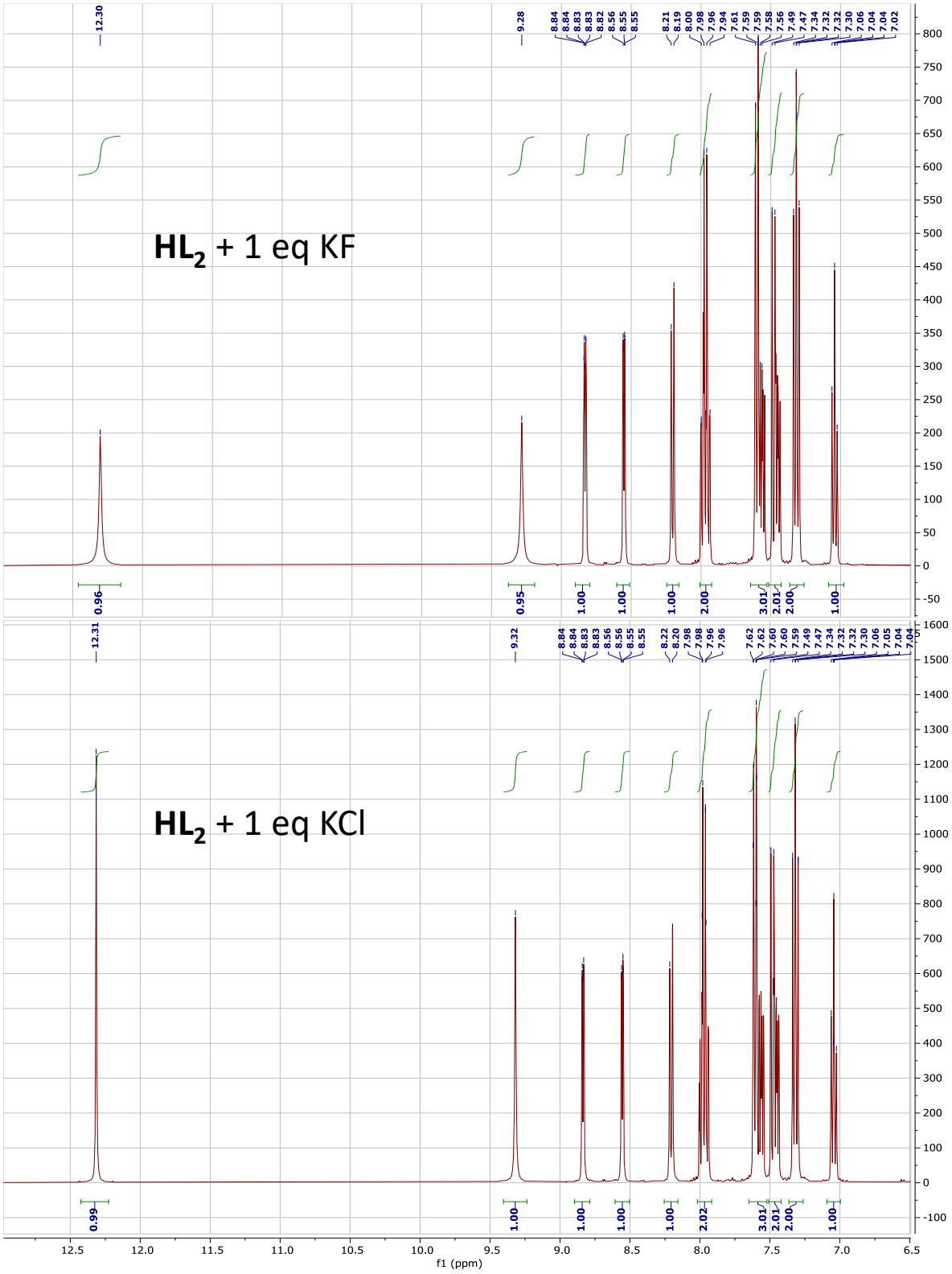

Fig. S11: ^{1}H-NMR spectra (DMSO-d_6, 400 MHz) of **HL_2** in presence of one equivalents of anions.

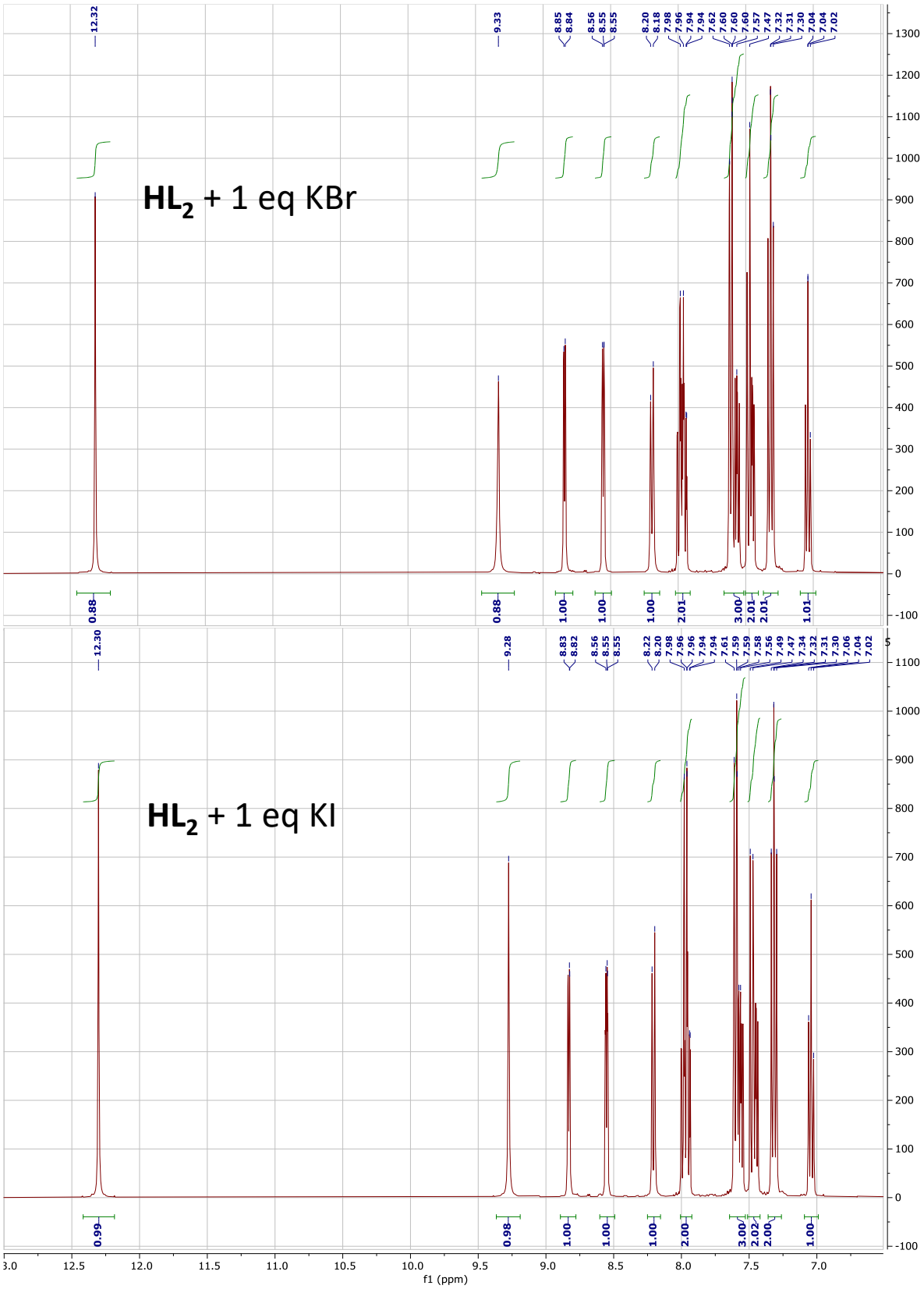

Fig. S12: ^{1}H-NMR spectra (DMSO-d_6, 400 MHz) of **HL_2** in presence of one equivalents of anions.

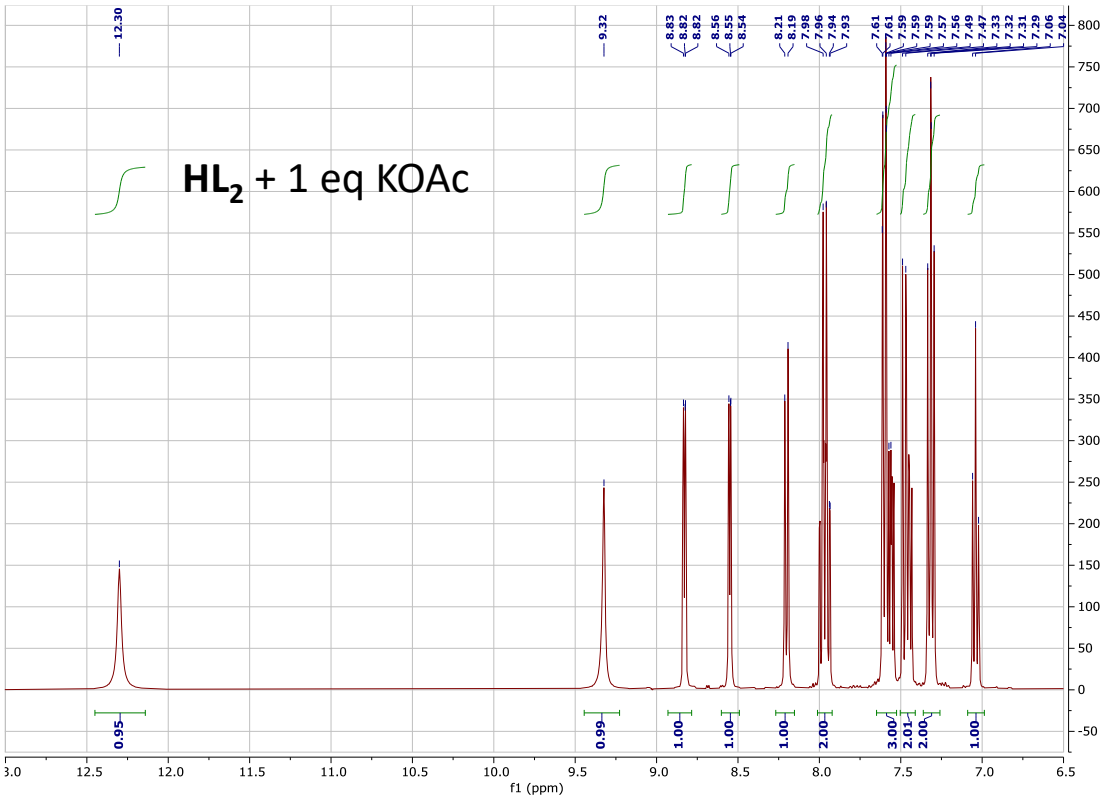

Fig. S13: ^{1}H-NMR spectra (DMSO-d_6, 400 MHz) of **HL_2** in presence of one equivalents of acetate anion.

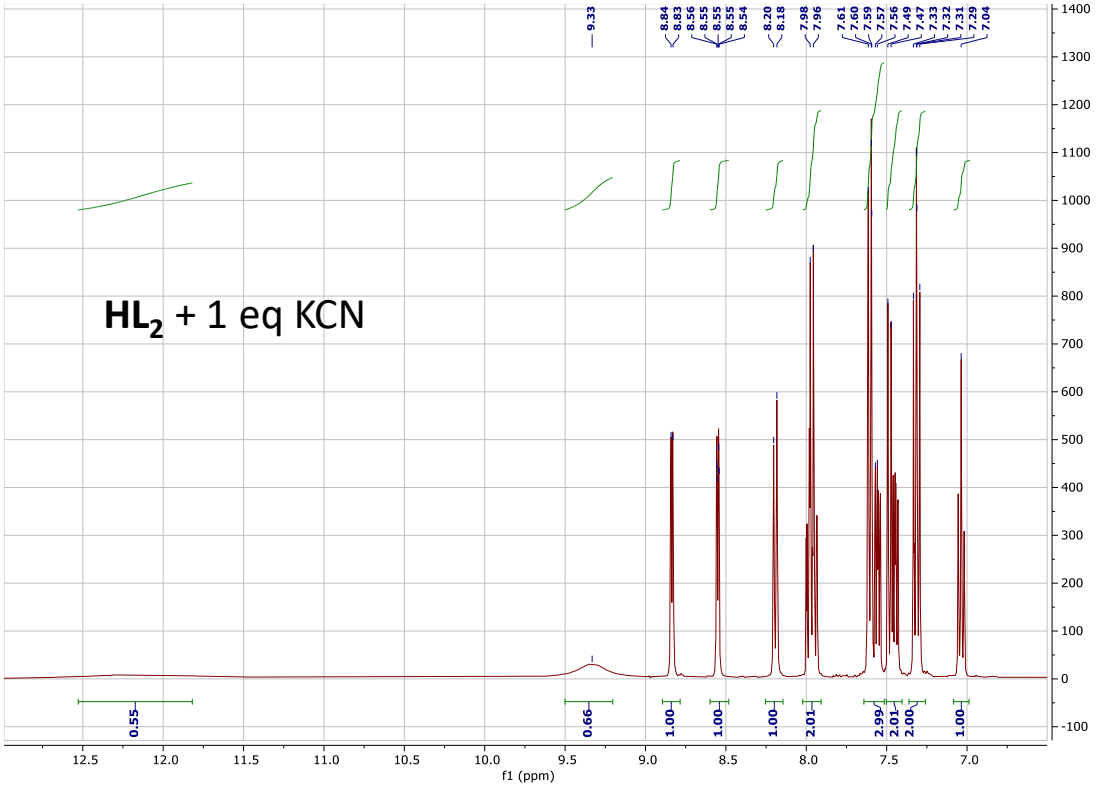

Fig. S14: ^{1}H-NMR spectra (DMSO-d_6, 400 MHz) of **HL_2** in presence of one equivalents of cyanide anion.

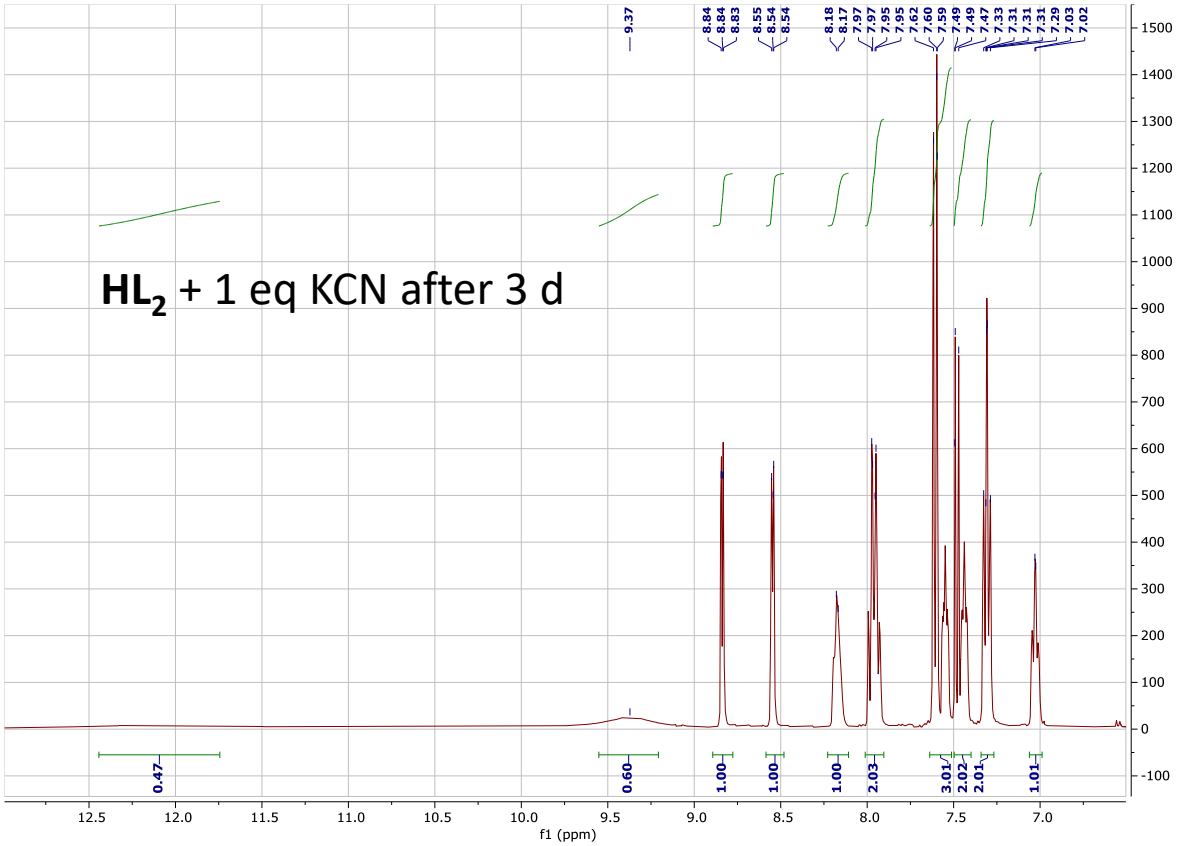

Fig. S15: ^{1}H-NMR spectra (DMSO-d_6, 400 MHz) of **HL_2** in presence of one equivalents of cyanide after 3 days.

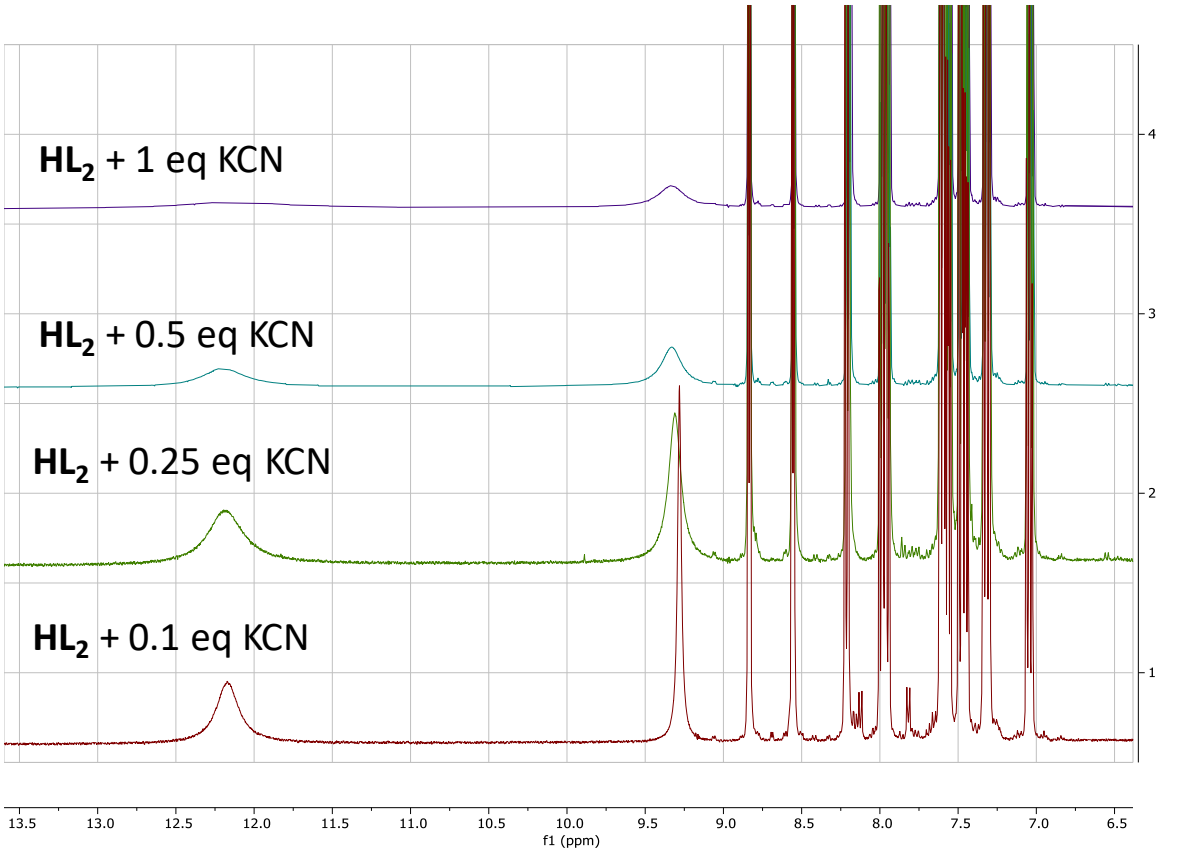

Fig. S16: ^{1}H-NMR spectra (DMSO-d_6, 400 MHz) of **HL_2** in presence of various equivalents of KCN.

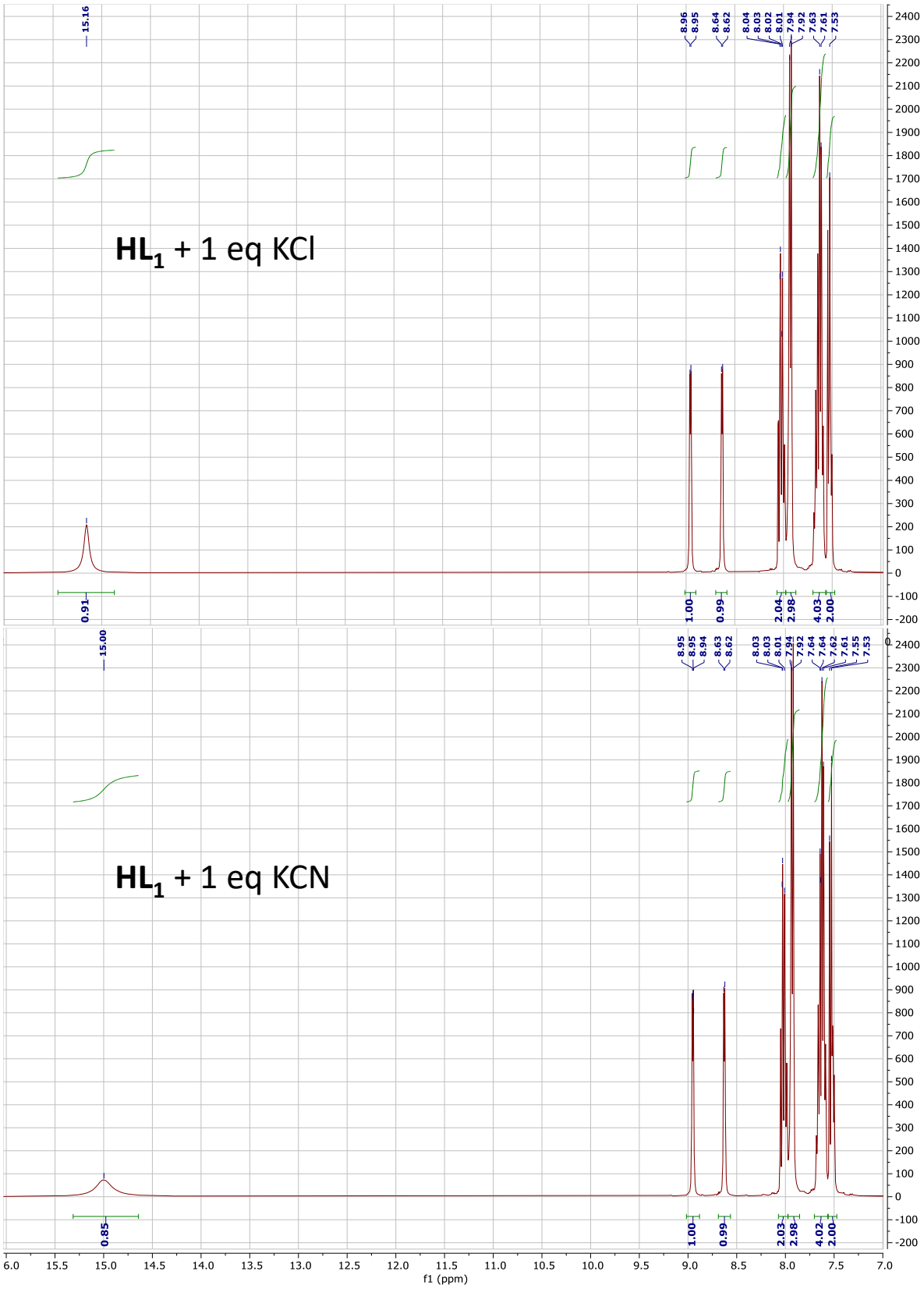

Fig. S17: ^{1}H-NMR spectra (DMSO-d_6, 400 MHz) of **HL_1** in presence of one equivalents of anions.

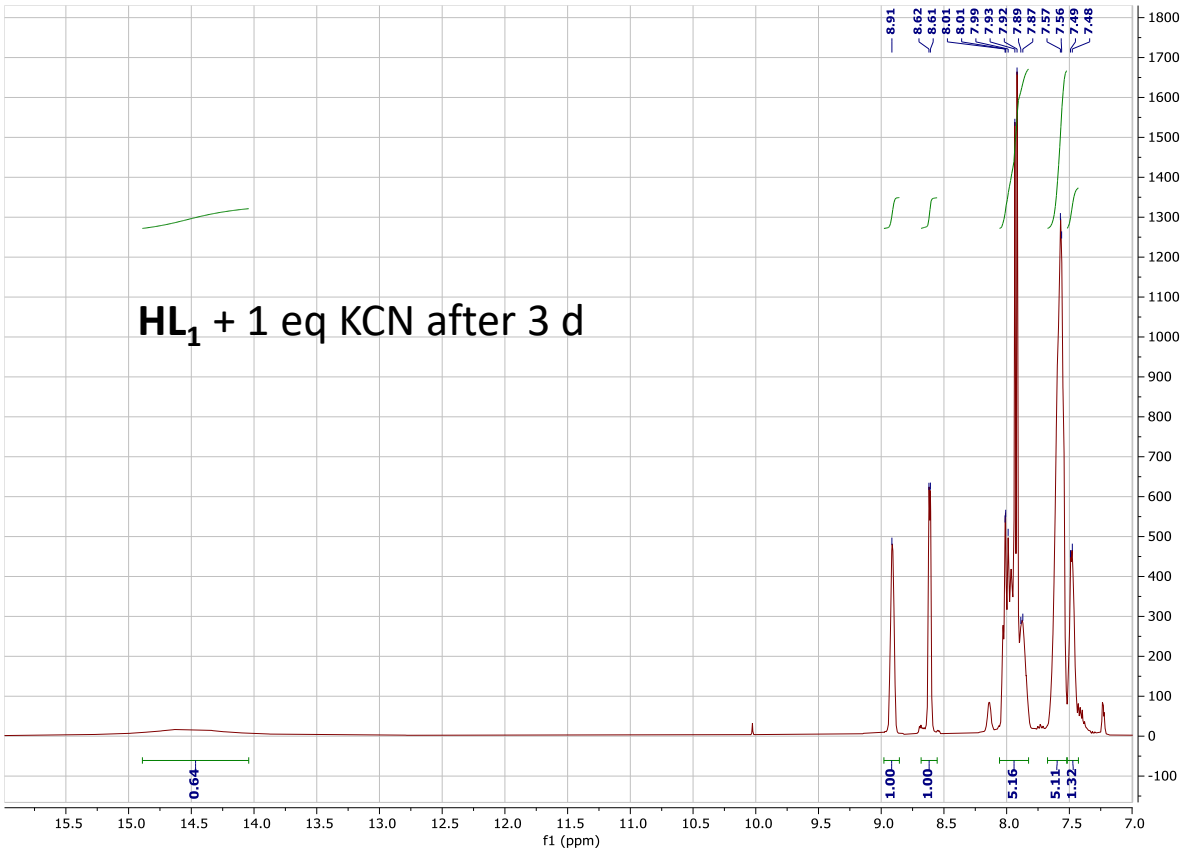

Fig. S18: ^{1}H-NMR spectra (DMSO-d_6, 400 MHz) of **HL_1** in presence of one equivalents of cyanide after 3 days.

5. Rheology

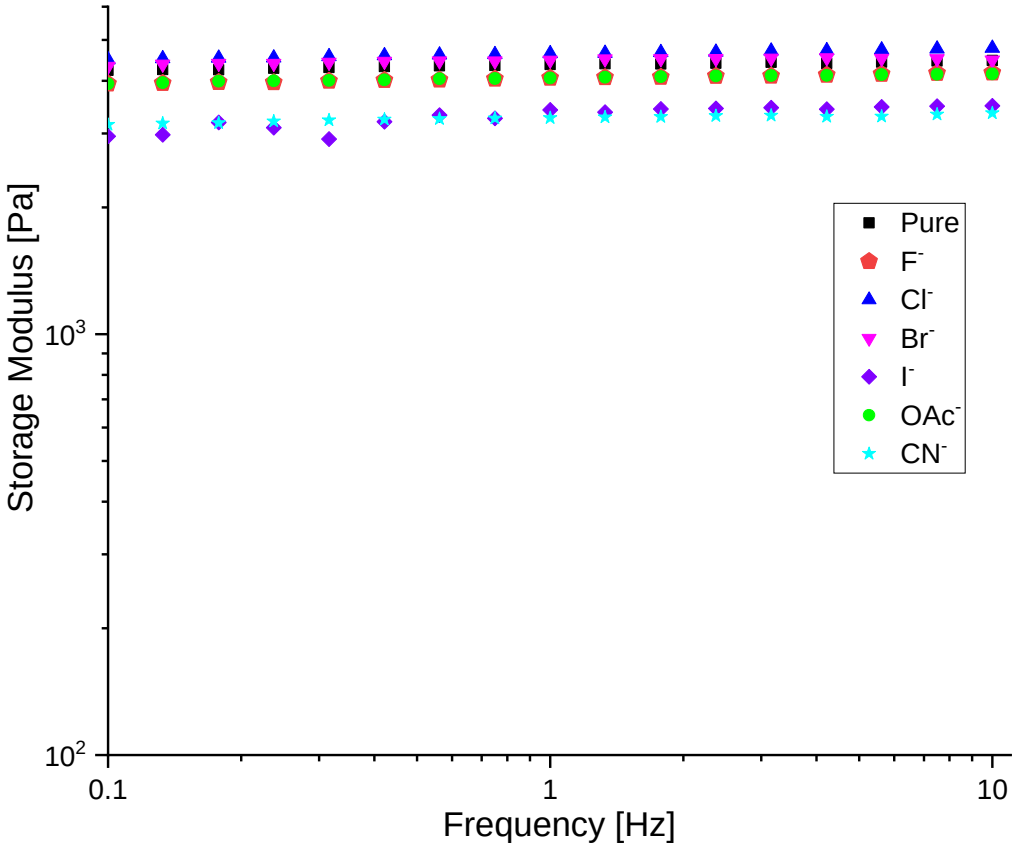

Fig. S19: Oscillatory frequency sweeps for **HL_2** at 1.0 wt%, in presence of three equivalents of anions in DMSO/water (1:1, v/v).

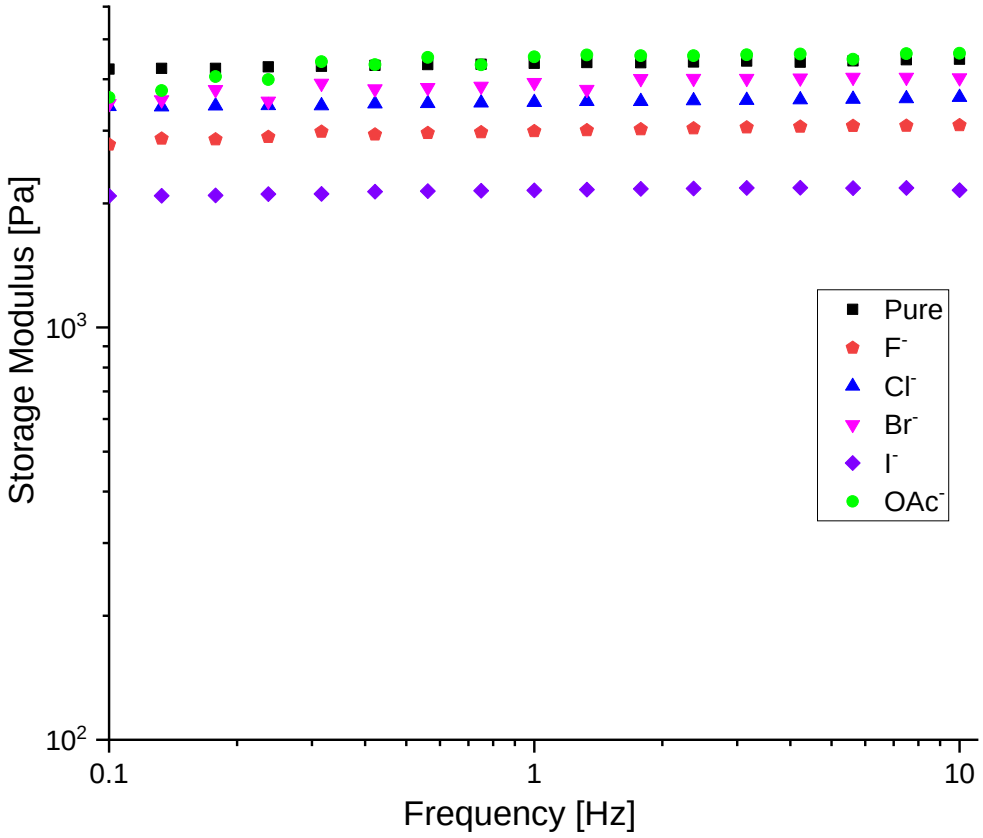

Fig. S20: Oscillatory frequency sweeps for **HL_2** at 1.0 wt%, in presence of six equivalents of anions in DMSO/water (1:1, v/v). The gel was broken in presence of six equivalents of cyanide.

6. IR spectroscopy

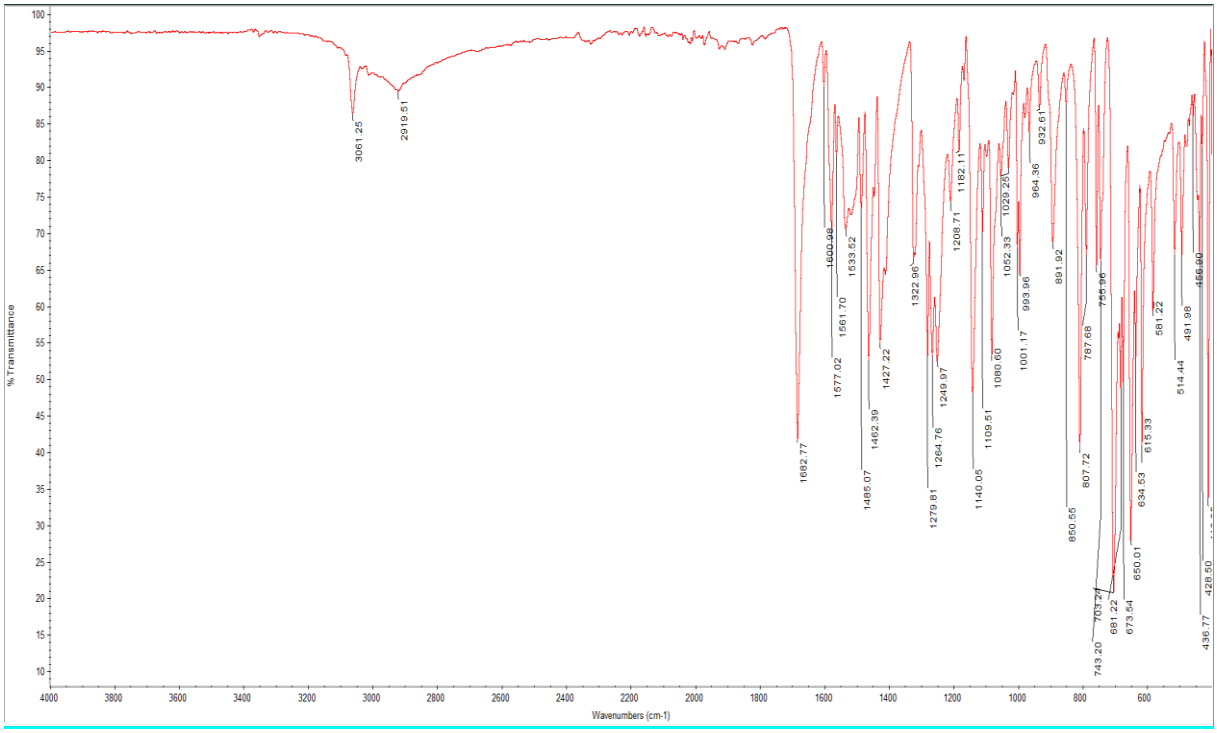

Fig. S21: ATR-FTIR spectra of **HL_1** bulk solid.

Fig. S22: ATR-FTIR spectra of **HL_1** xerogel obtained from DMSO/water (1:1 v/v) at 5.0 wt%.

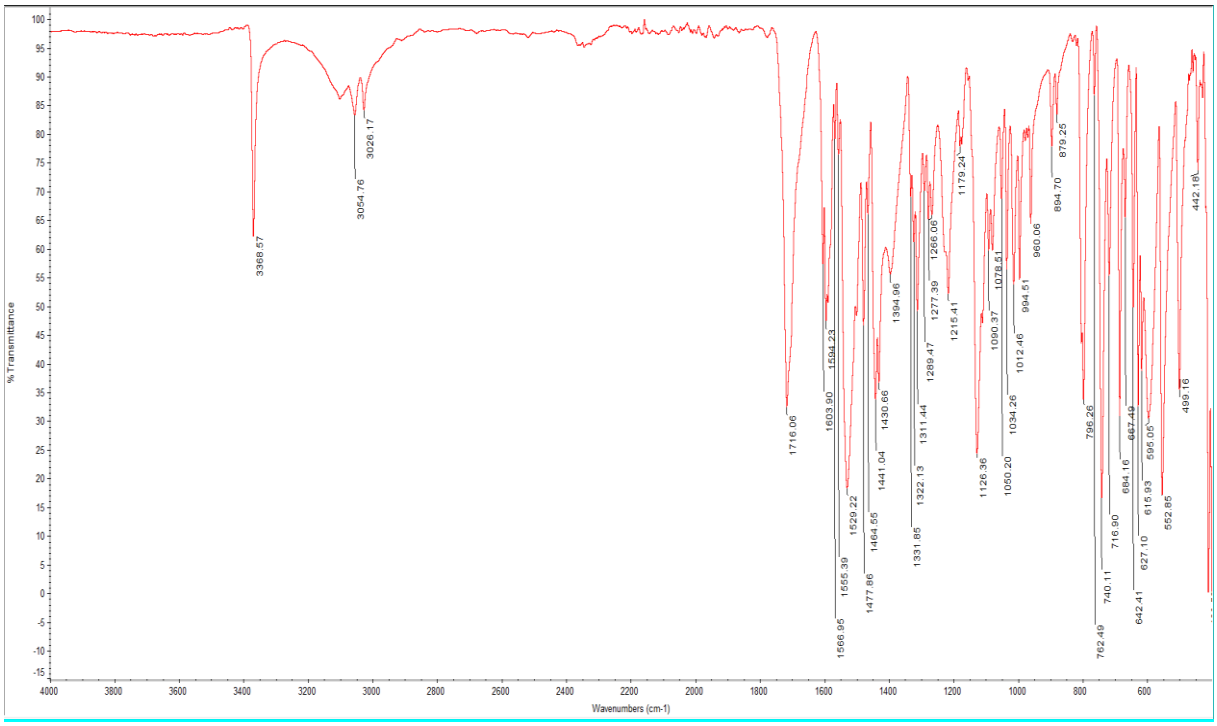

Fig. S23: ATR-FTIR spectra of **HL_2** bulk solid.

Fig. S24: ATR-FTIR spectra of **HL_2** xerogel obtained from DMSO/water (1:1 v/v) at 5.0 wt%.

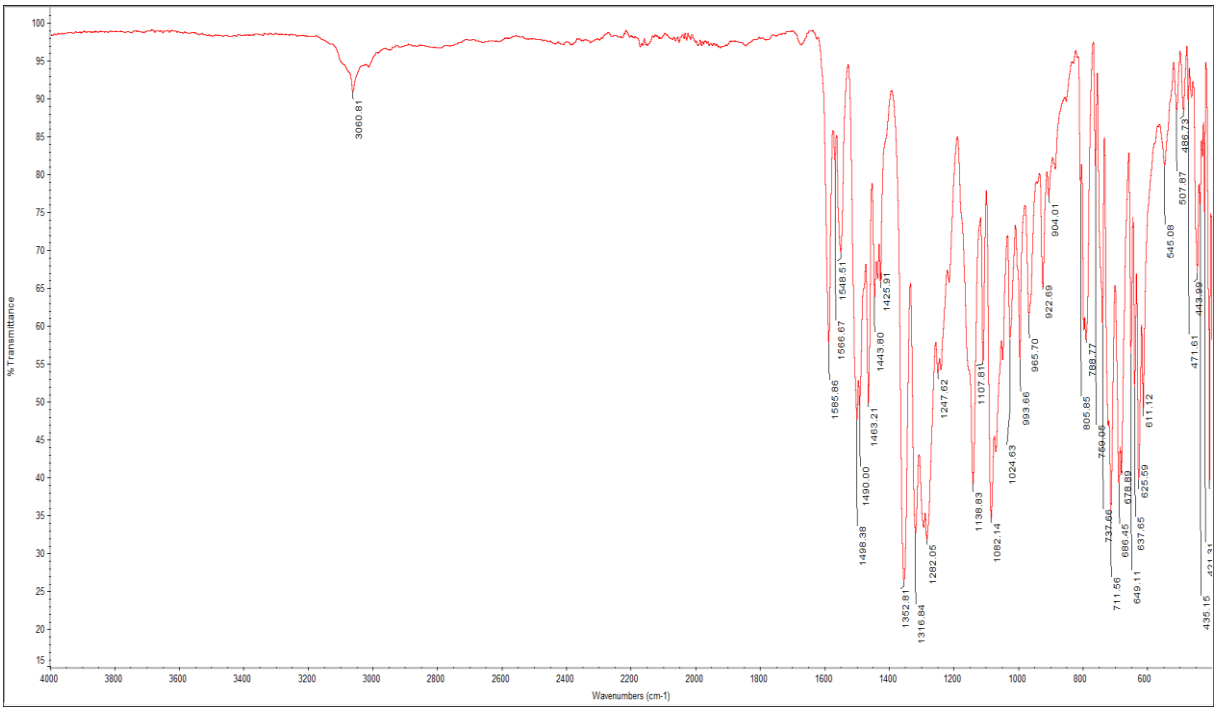

Fig. S25: ATR-FTIR spectra of complex **1** (crystals).

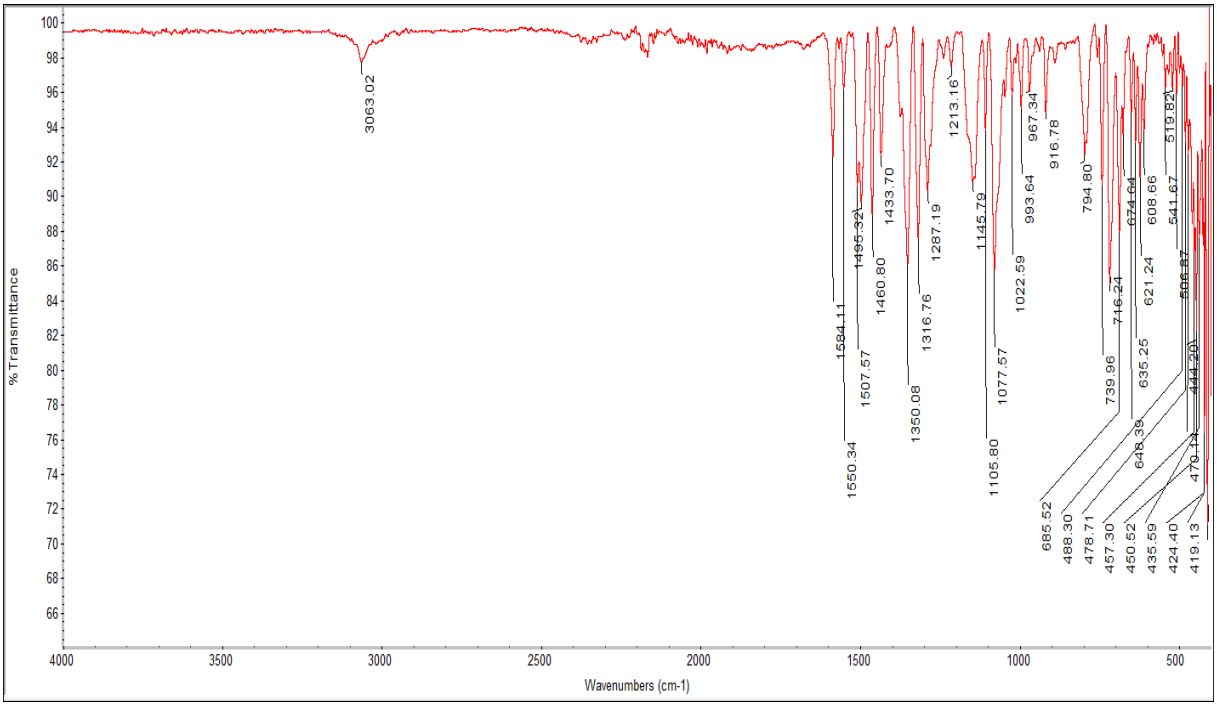

Fig. S26: ATR-FTIR spectra of complex **2** (crystals).

Fig. S27: ATR-FTIR spectra of complex **4** (crystals).

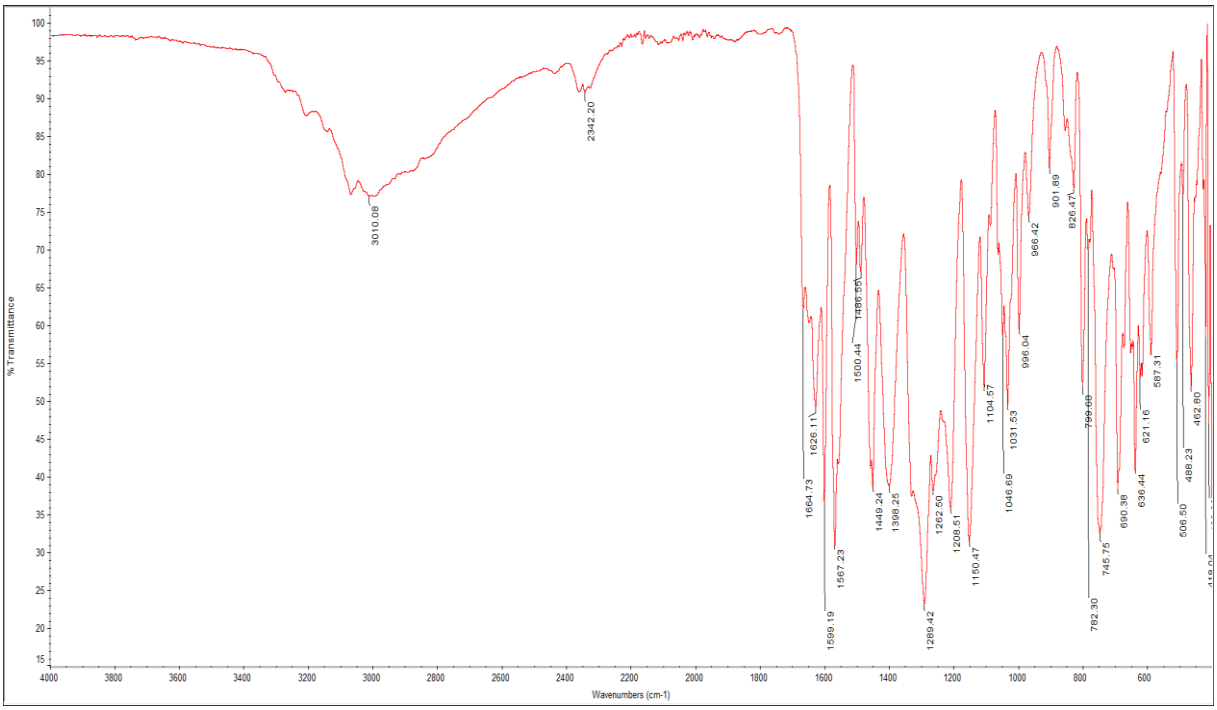

Fig. S28: ATR-FTIR spectra of complex **5** (crystals).

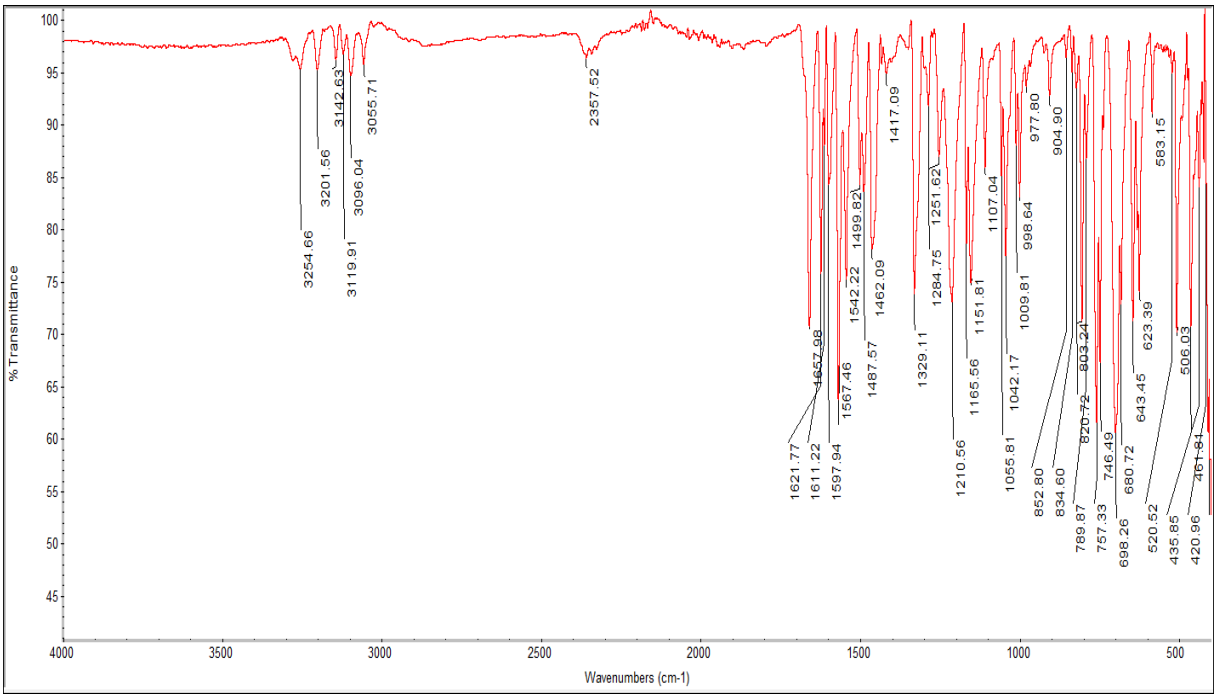

Fig. S29: ATR-FTIR spectra of complex **7** (crystals).

Table S5: IR-peaks of the ligand and metal complexes.

Compound	C=O stretching (cm^{-1})
HL_1, bulk solid	1682
HL_1, xerogel	1682
HL_2, bulk solid	1716
HL_2, xerogel	1715
Complex 1, crystal	1585
Complex 2, crystal	1584
Complex 4, crystal	1584
Complex 5, crystal	1626, 1664
Complex 7, crystal	1658

7. X-ray powder diffraction

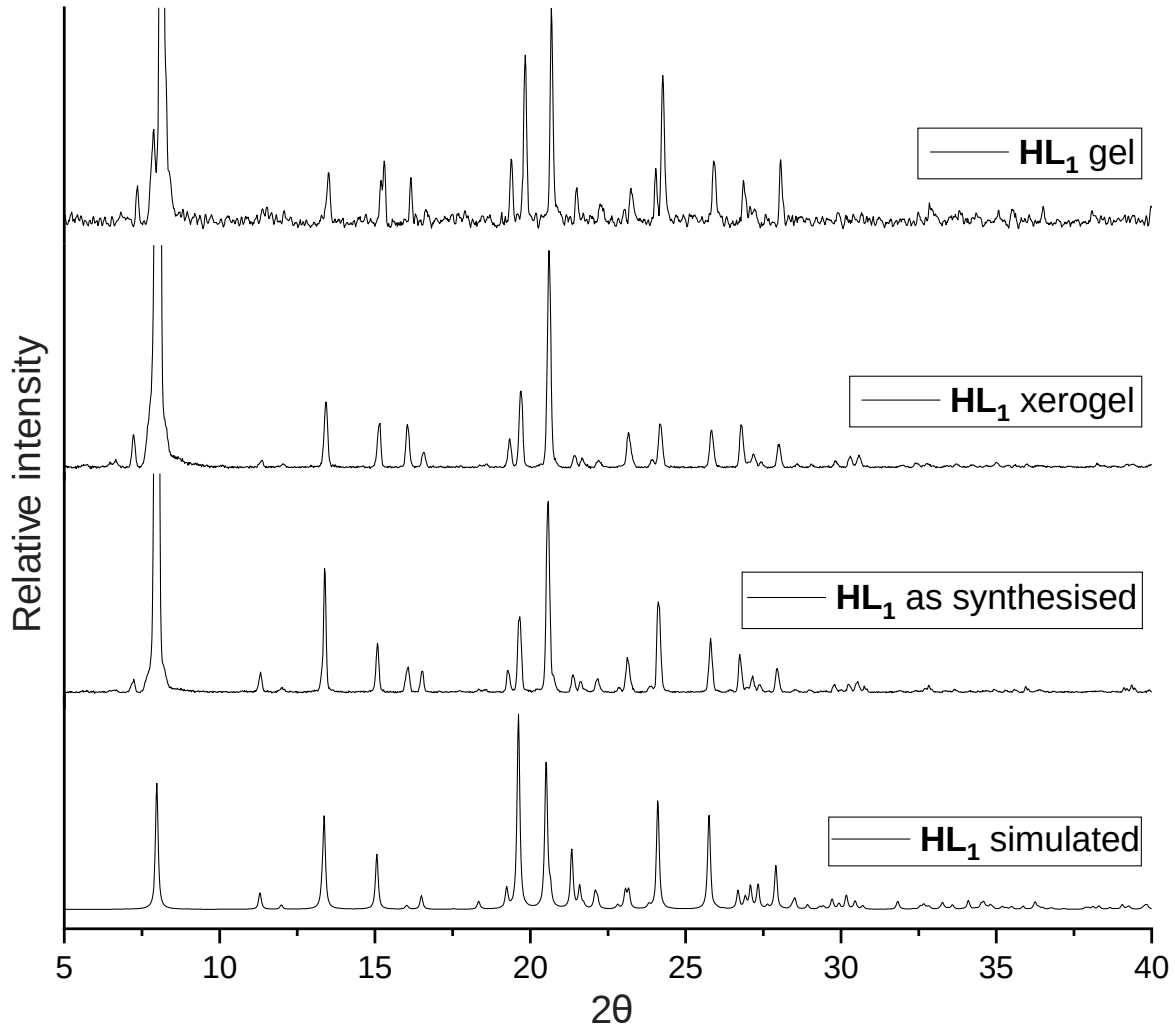

Fig. S30: XRPD comparison of **HL_1**: simulated pattern obtained from single-crystal data, bulk solid, and xerogel/gel obtained from DMSO/water (1:1 v/v) at 5.0 wt%. The Y-axis was adjusted in bulk solid and xerogel graphs due to high intensity of the peak at $2\theta \approx 8$.

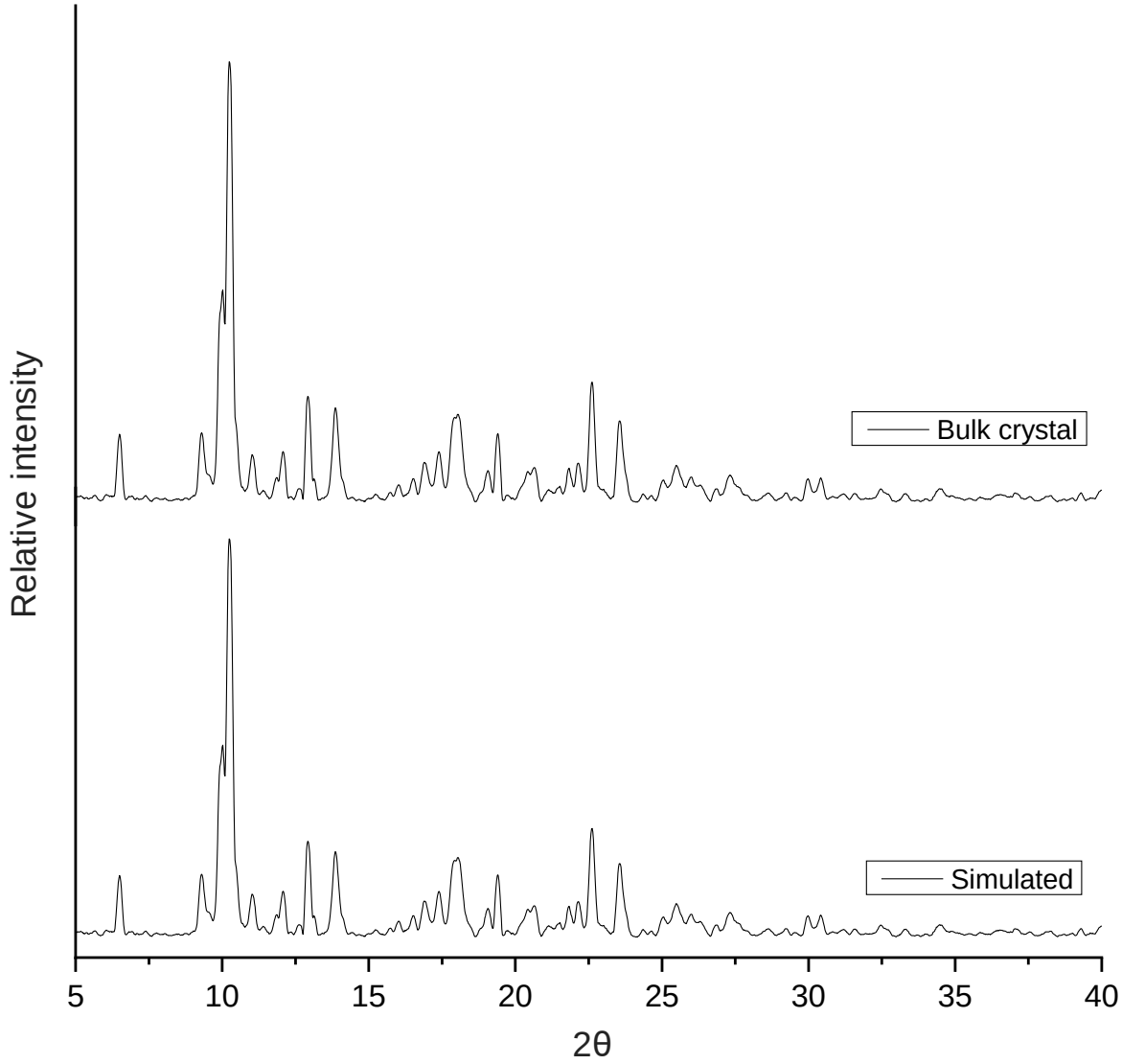

Fig. S31: XRPD comparison of complex **1**: simulated pattern obtained from single-crystal data (bottom) and bulk crystal (top) obtained from DMF/water (1:1 v/v).

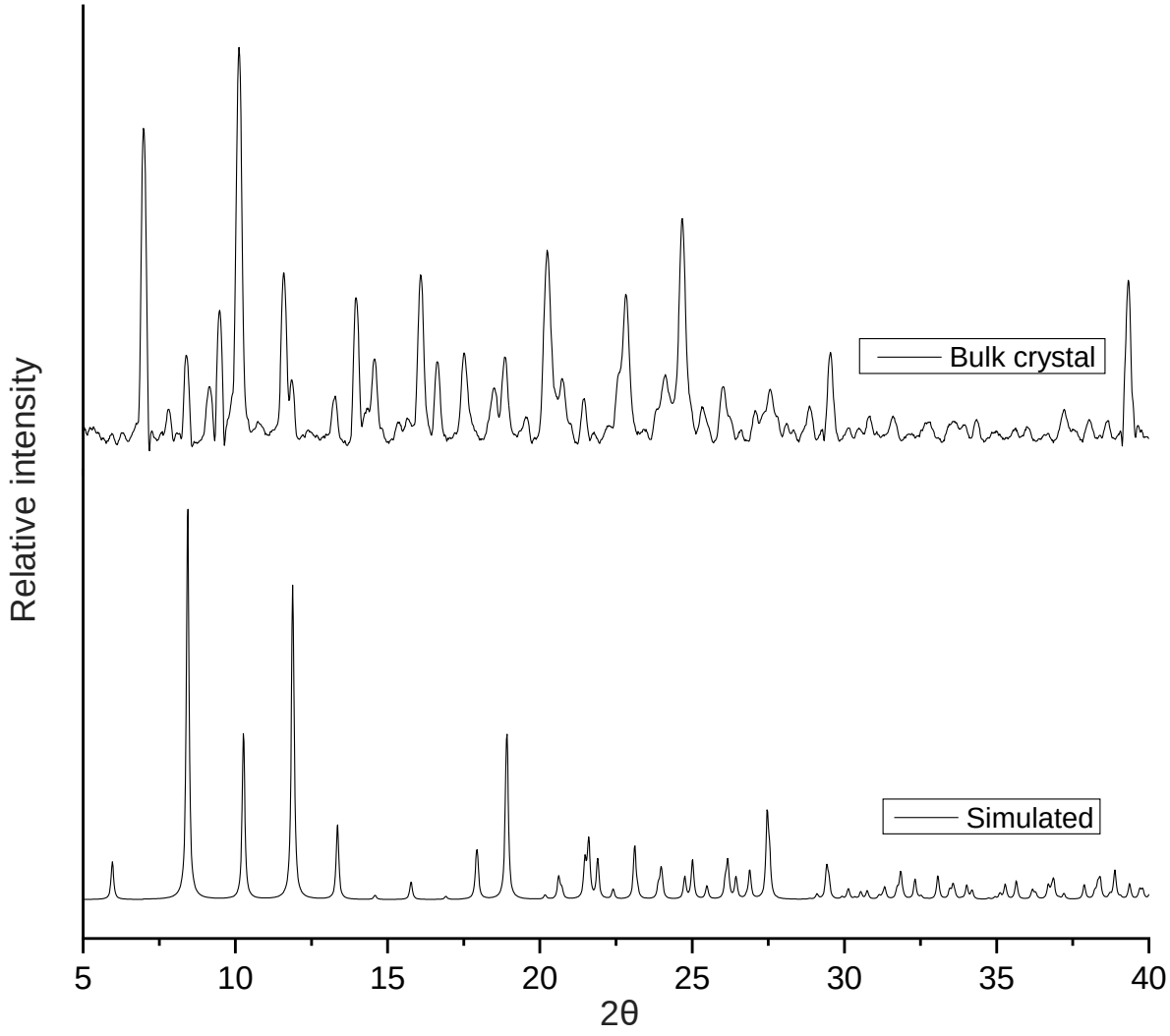

Fig. S32: XRPD comparison of complex **2**: simulated pattern obtained from single-crystal data (bottom) and bulk crystal (top) obtained from DMF/water (7:3 v/v).

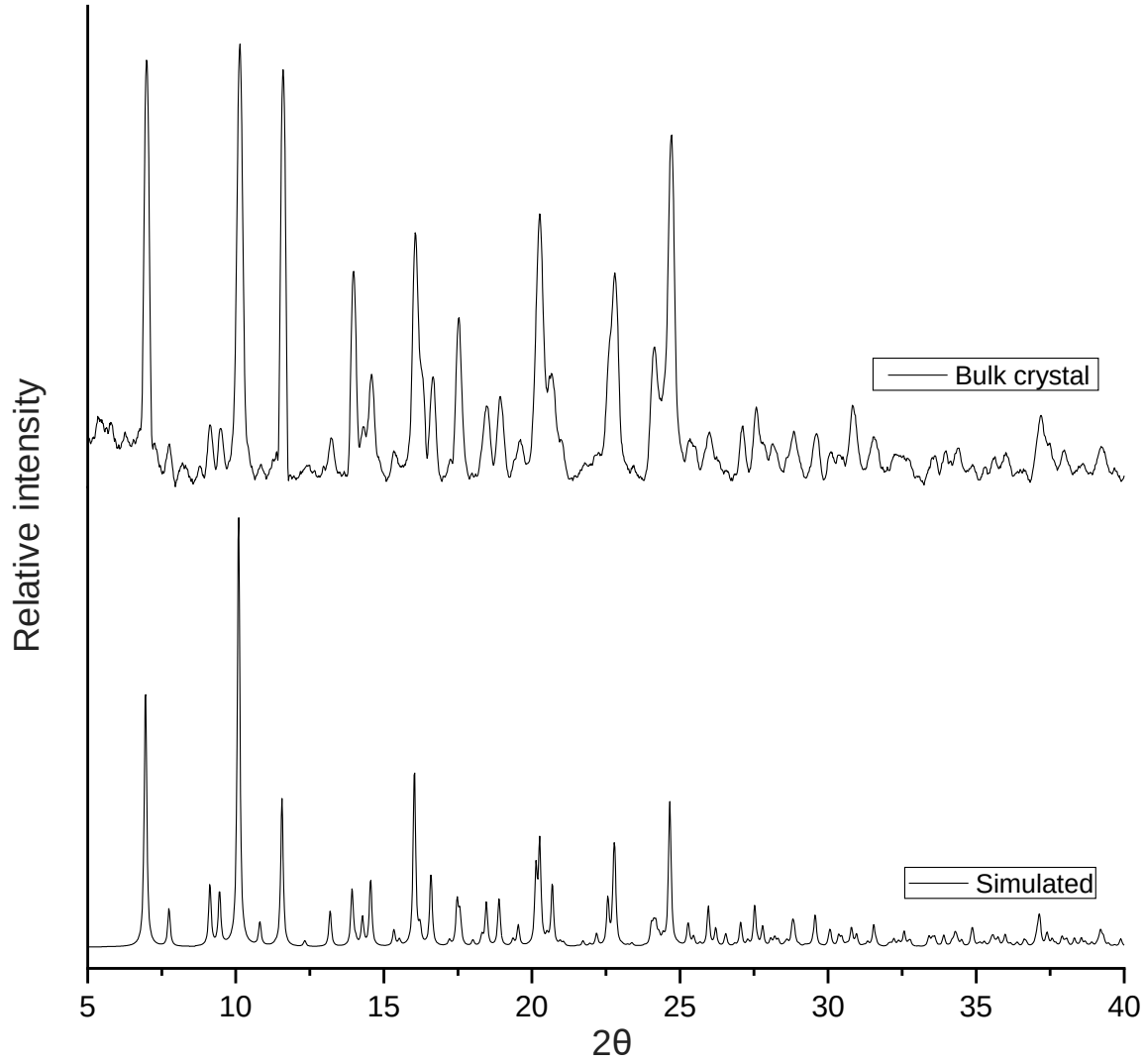

Fig. S33: XRPD comparison of complex **4**: simulated pattern obtained from single-crystal data (bottom) and bulk crystal (top) obtained from DMF/water (1:1 v/v).

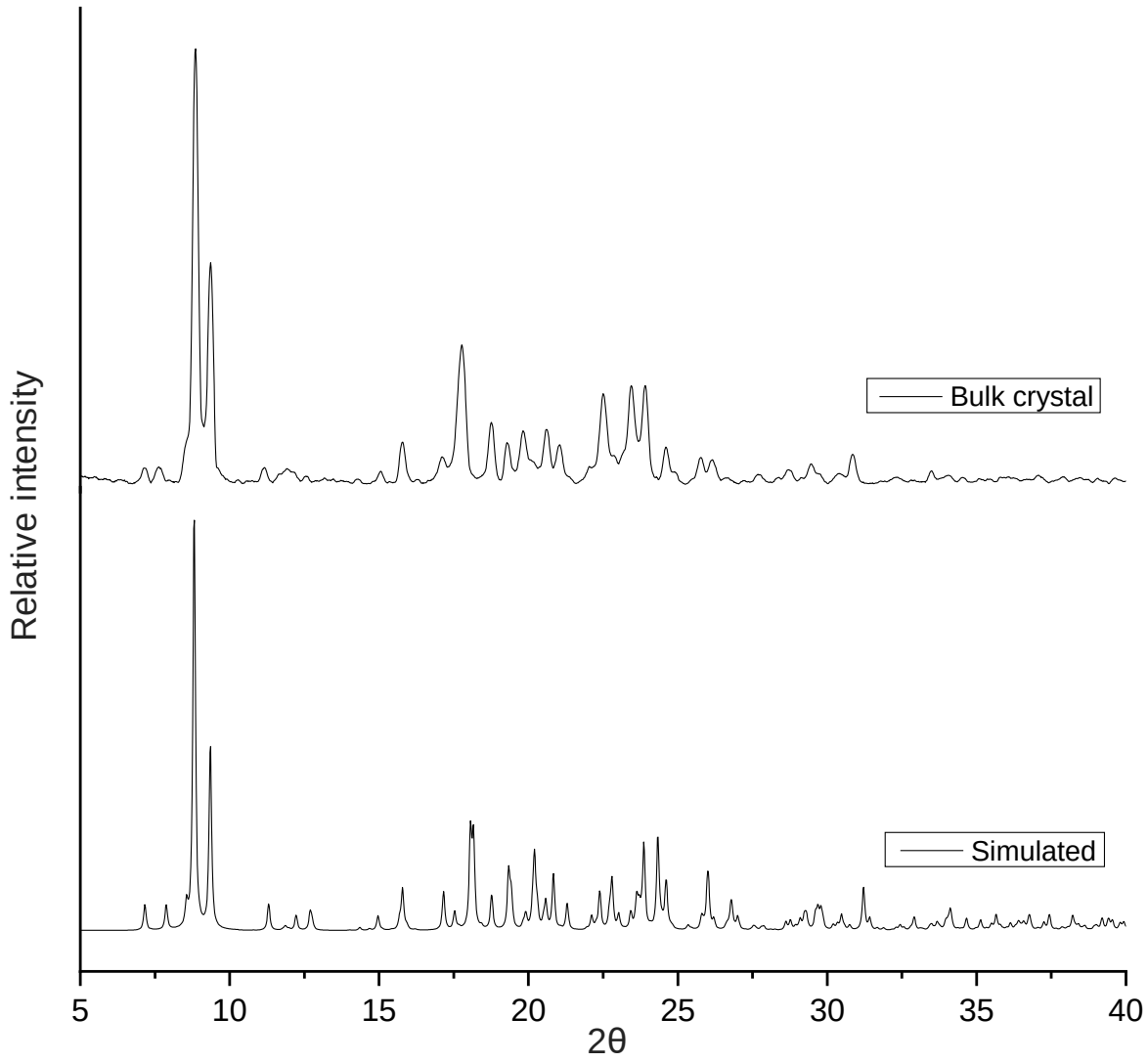

Fig. S34: XRPD comparison of complex **5**: simulated pattern obtained from single-crystal data (bottom) and bulk crystal (top) obtained from MeOH.

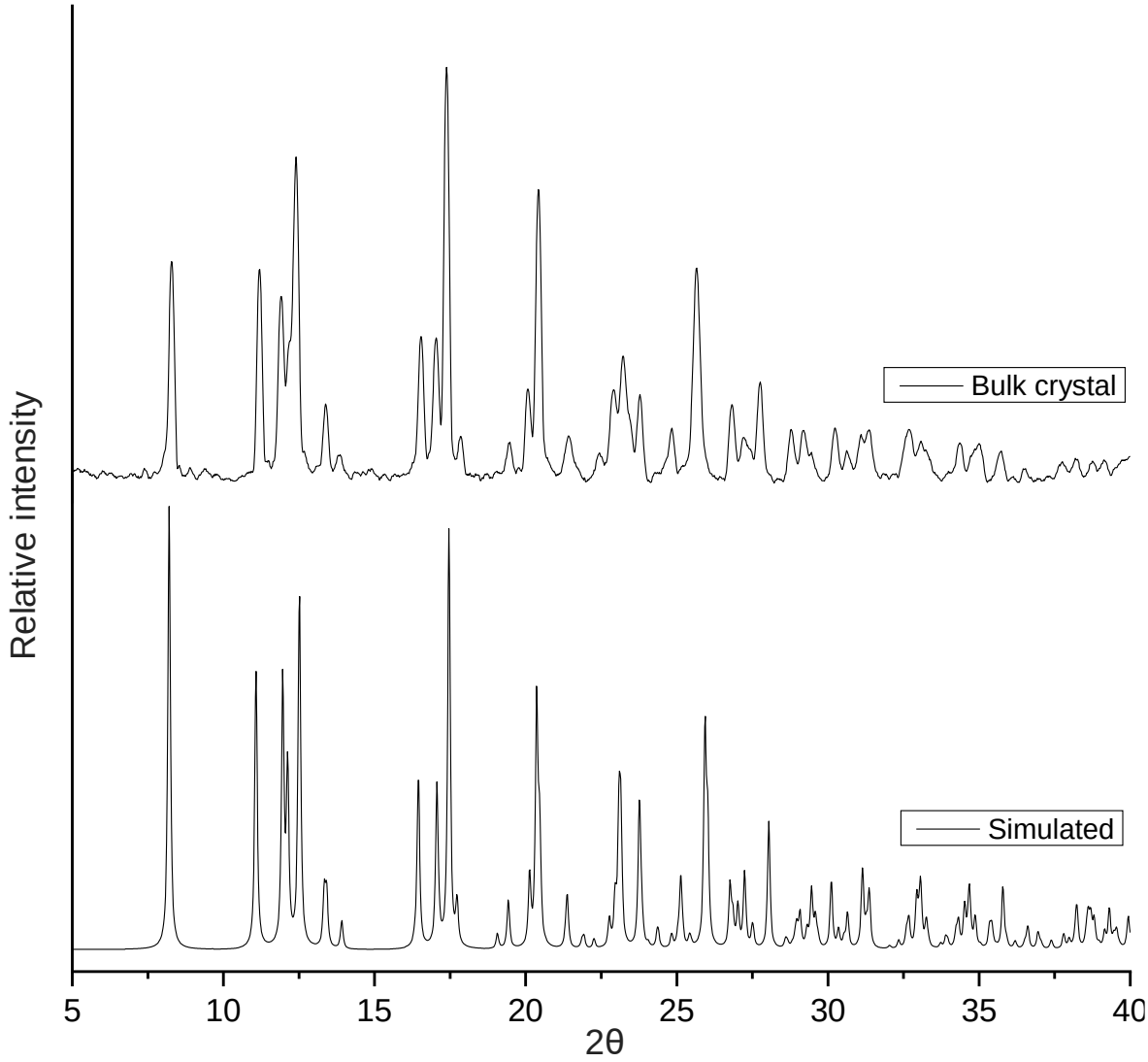

Fig. S35: XRPD comparison of complex **7**: simulated pattern obtained from single-crystal data (bottom) and bulk crystal (top) obtained from DMF/water (1:1 v/v).

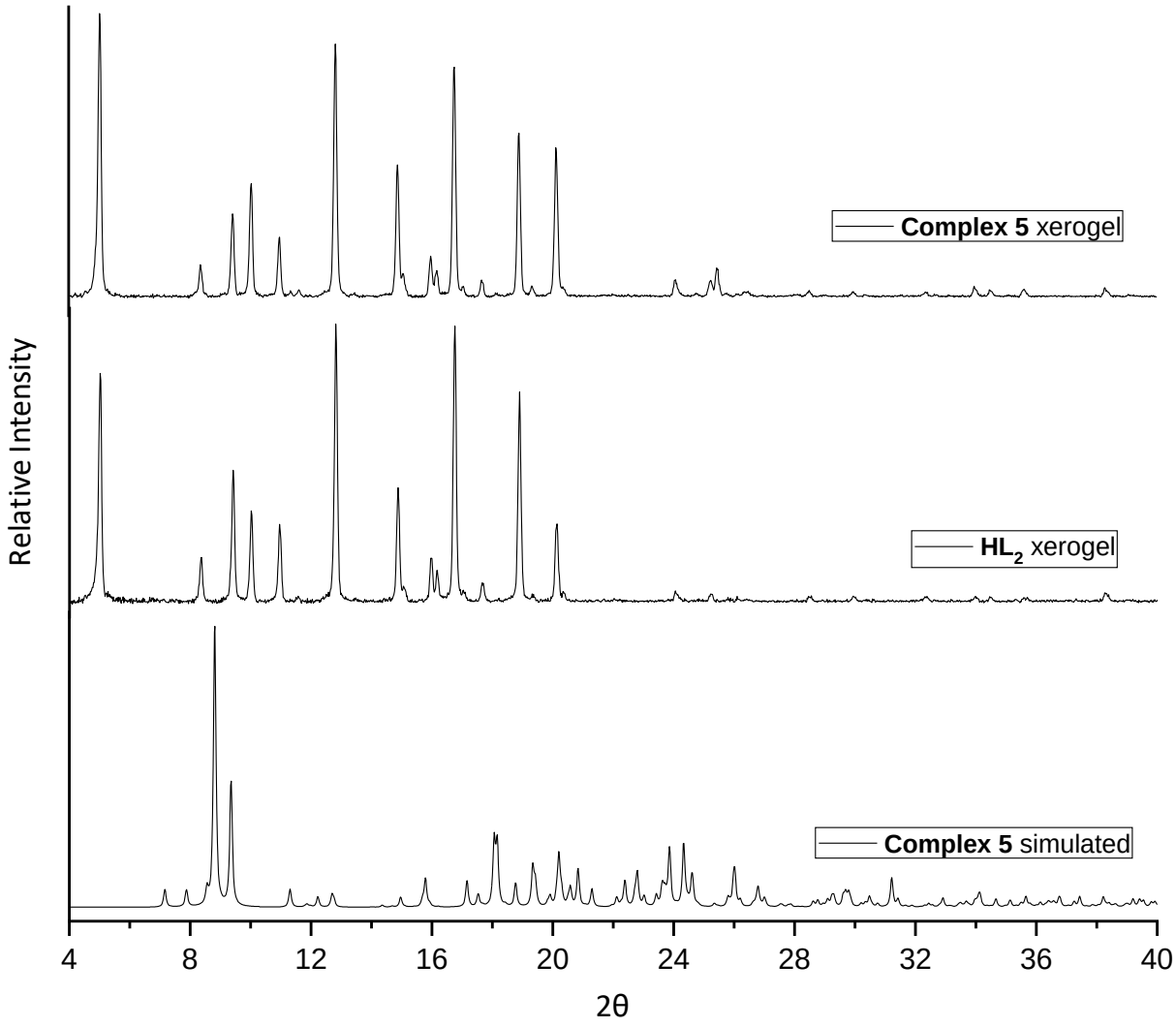

Fig. S36: XRPD comparison of simulated pattern of complex **5** obtained from single-crystal data (bottom), xerogel of **HL_2** (middle) obtained from DMF/water (1:1 v/v) at 1.0 wt% and xerogel of **complex 5** (top) obtained from DMF/water (1:1 v/v) at 2.5 wt% showing the decomposition of the metal complex.